Group 10 Metal Complexes of SPS-Based Pincer Ligands: Syntheses, X-ray Structures, and DFT Calculations

Marjolaine Doux,[a] Nicolas Mézailles,[a] Louis Ricard,[a] and Pascal Le Floch*[a]

Keywords: Phosphorus / S ligands / Donor-acceptor systems / Density functional calculations / Group 10 elements

The 2,6-bis(diphenylphosphanylsulfide)phosphinine (**1**) reacts with water to afford a 1,2-dihydrophosphinine oxide **5** featuring a P–H bond. Reaction of **5** with one equivalent of $[Pd(COD)Cl_2]$ yields the SPS pincer-based complex **6** with a P(OH) λ^5-phosphinine central ligand. Complex **6** has been structurally characterized. Two possible mechanisms account for the formation of **5**: an intramolecular P–H to P–Pd metathesis or one based on the P=O to POH equilibrium. Methanol, ethanol or diethylamine also react with **1** to afford the corresponding P(H)(OMe) **7**, P(H)(OEt) **8**, and P(H)(NEt_2) **9** λ^5-phosphinines. No definitive mechanism for the formation of **7**–**9** can be proposed since no intermediates were detected in situ by ^{31}P NMR spectroscopy. However, DFT calculations (at the B3LYP 6-311+G(d,p) level of theory) suggest that the conversion of 1,2-dihydrophosphinines into λ^5-phosphinines is not viable because it involves a high activation energy. Like **5**, λ^5-phosphinines **7** and **8** react with $[Pd(COD)Cl_2]$ to afford the expected palladium complexes **10** and **11**. An alternative method relies on the reactivity of nucleophiles with a SPS pincer-based complex **2** featuring a P–Cl bond. (–)-Menthol and lithium diethylamide react with **2** to yield the expected P-OMen **13** and P-NEt_2 **14** complexes. Both complexes have been structurally characterized. Bromonickel **18** and chloroplatinum **19** complexes of the SPS ligand, featuring a P–Br or P–Cl bond, have also been prepared by reacting **1** with $[NiBr_2(DME)]$ and $[Pt(COD)Cl_2]$, respectively. Like their palladium congener, both species react with ethanol to afford the corresponding P–OEt derivatives **20** [M = Ni] and **21** [M = Pt]. *n*Butyl derivatives of these SPS ligands also bind to Ni–Br (complex **22**) and Pt–Cl (complex **23**) fragments. Both complexes were straightforwardly prepared by reacting anion **3**, resulting from the reaction of *n*BuLi with **1**, with the $[NiBr_2(DME)]$ and $[Pt(COD)Cl_2]$ precursors. The chloride ligand is readily substituted by acetonitrile in complexes **4**, **11**, **20**, and **21** upon treatment with $AgBF_4$ in dichloromethane. Reaction of AgOTf with the palladium complex **4** affords complex **28** via substitution of the chloride ligand by TfO^-. The X-ray crystal structures of the dimethyl-λ^5 derivative **29** of **1**, and that of its P-OMe anion **30**, have been recorded. Anion **30** can be regarded as a phosphanyl-substituted pentadienyl anion. DFT calculations and a charge decomposition analysis (CDA) show that the phosphorus atom in these SPS-pincer structures is a classical tertiary phosphane ligand in terms of donation and acceptance.

Introduction

The last decade has seen considerable interest in the synthesis and use of pincer ligands in coordination chemistry and catalysis, largely due to their particular backbone that allows not only the meridional encapsulation of transition metals but also the fine tuning of their coordination behavior and electronic capacity by varying the central or ancillary ligands. This area, pioneered by Shaw,[1] has been thoroughly reviewed recently.[2−4] Though early studies mainly focused on the ubiquitous PCP systems, polyheteroatomic-based pincer ligands featuring N, O, P, and S atoms have attracted increasing attention because multiple combinations can be used to build mixed systems.[5−7] Sulfur-based ligands are particularly appealing since they can also be employed in the elaboration of synthetic models of enzymes.[8] Mainly, four types of sulfur ligands are used: classical thioethers,[9−12] thiolates,[13,14] sulfoxides,[15] in which coordination occurs through the remaining lone pair at sulfur, and phosphane sulfides.[16,17] The latter, though not yet employed in pincer type structures, have found an interesting application in the rhodium-catalyzed carbonylation of methanol when incorporated in a mixed P−P=S bidentate ligand.[18,19]

Conversely, phosphane derivatives (probably the most studied ligands) have essentially been used as peripheral binding sites in pincer systems. This clearly results from their tetrahedral geometry that precludes the elaboration of planar rigid-backbones when the phosphorus atom is the central ligand. Therefore, the building of pincer systems incorporating a planar phosphorus atom as central binding site is an interesting challenge. Besides their structural interest, such systems exhibit very peculiar electronic properties that markedly differ from those of classical phosphanes and

[a] Laboratoire "Hétéroéléments et Coordination", UMR CNRS 7653 (DCPH), Département de Chimie, Ecole Polytechnique, 92128 Palaiseau Cédex, France
Fax: (internat.) +33-1-69333990
E-mail: lefloch@poly.polytechnique.fr
Supporting information for this article is available on the WWW under http://www.eurjic.org or from the author.

  DOI: 10.1002/ejic.200300303

nitrogen analogs. Indeed, phosphorus in multiple bonds essentially behaves as a relatively poor σ-donor ligand but displays a powerful π-accepting capacity.[20] Very different systems, incorporating phosphaalkene (P analogs of alkenes) or heterocycles, can be anticipated but, in practice, only aromatic phosphorus heterocycles are sufficiently stable.

We thus recently launched a program aimed at incorporating phosphinines (phosphorus analogs of pyridines) in pincer-type structures. Our initial work focused on the synthesis of mixed S-P-S ligands featuring a phosphinine as central unit and two phosphane sulfides as ancillary ligands. Such systems proved to be easily available in large amounts by sulfurization of the corresponding 2,6-bis(diphenylphosphanyl)-λ^3-phosphinines. However, the highly electropositive phosphorus atoms are particularly reactive towards nucleophilic attack. Thus the reaction of ligand **1** with [Pd(COD)Cl_2] afforded a complex **2** featuring a central (λ^5-σ^4) pentavalent tetracoordinate phosphorus atom.[21] This new type of palladium complex, which can be derivatized by nucleophilic displacement of the chlorine atom at phosphorus, is particularly stable. Recently, we devised a much more rational approach to these complexes through the reaction of 1-*R*-1-*P*-phosphahexadienyl anions with [Pd(COD)Cl_2]. Thus, anion **3**, which is readily obtained by reacting *n*BuLi with phosphinine **1**, reacted with [Pd(COD)Cl_2] to afford complex **4** (Scheme 1). The latter proved to be particularly active (TON up to 10000) in the Miyaura-catalyzed cross-coupling process that allows the synthesis of aromatic boronic esters from halo aromatic and dialkoxyboranes.[22]

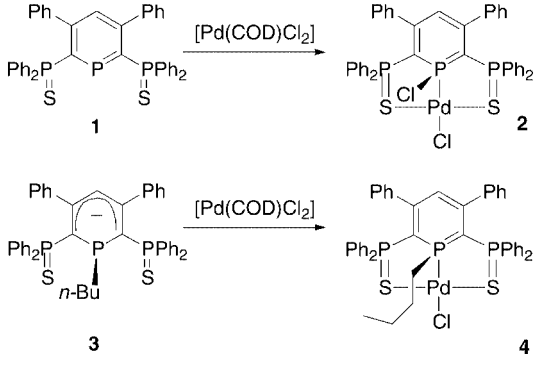

Scheme 1

As this chemistry might be extended to other metal centers, we aimed to expand the synthesis of this new type of phosphorus ligand and their applications in coordination chemistry and catalysis. We report here the synthesis of group 10 metal complexes. Different synthetic methodologies, the X-ray structures of some complexes as well as a preliminary theoretical study of their electronic properties are reported.

Results and Discussion

Two routes that exploit the high electrophilicity of the phosphorus atom in **1** have already been designed for the synthesis of these SPS palladium complexes. In exploring the reactivity of **1** toward nucleophiles, we found that reaction with water readily afforded the 1,2-dihydrophosphinine oxide **5** (Scheme 2). This is a common transformation for non-kinetically stabilized phosphaalkenes, but not, usually, for λ^3 -phosphinines in which the P=C double bond is thermodynamically stabilized.[23,24] However, the presence of strong acceptor groups at the α position of phosphorus (C2 and C6) sometimes provokes a significant dearomatization of the ring.[25] Interestingly, only one diastereomer of **5** was formed. The mechanism leading to **5** is discussed below.

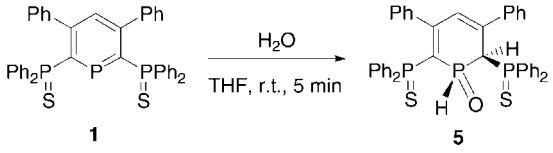

Scheme 2

The structure of **5**, fully characterized by NMR spectroscopy and elemental analysis, was confirmed by an X-ray crystal structure study. It shows no particular features and is not presented here.[26] Interestingly, **5** could also be used as a source of [Pd(SPSOH)Cl] (**6**) [SPS = $C_5H(Ph_2PS)_2P$] upon reaction with [Pd(COD)Cl_2] (Scheme 3).

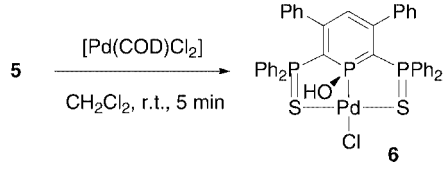

Scheme 3

Complex **6** was characterized by ^{31}P and ^{1}H NMR as well as by elemental data but was too insoluble to be characterized by ^{13}C NMR spectroscopy. Fortunately, suitable crystals for an X-ray crystal analysis could be grown by diffusing hexanes into a chloroform solution of the complex. A view of one molecule of **6** and the most significant metric parameters (Figure 1), and crystal data and structural refinement details (Table 6), are presented here. Complex **6** adopts a distorted planar geometry around the palladium atom and the two sulfides act as ancillary ligands. The most interesting data are the internal metric parameters within the SPS ligand. As previously noted for the *n*Bu derivative **4**, the phosphorus atom and the C3 carbon atom escape from the plane defined by the C1−C2−C4 and C5 atoms by 19.0° and 4.8°, respectively, to yield a boat-like conformation. Though the pyramidality of the phosphorus atom (316.5°) compares with that of classical tertiary phosphanes, the P−C1 [1.757(4) Å] and P−C5 [1.767(4) Å] bond lengths are very short. At first sight, these data suggest that the ylidic character of the λ^5-phosphinine has been pre-

served upon coordination. Another intriguing piece of data is the bond lengths within the two ancillary P=S ligands. Indeed, whereas the two external P−C bond lengths [e.g. P3−C5 = 1.776(4) Å] are also very short compared to classical P−C single bonds, the two P=S bonds are lengthened [e.g. P2−S1 = 2.039(2) Å] compared with classical uncoordinated and coordinated phosphane sulfides. For example, in [Pd(R_3P=S)] complexes the P=S bond length usually falls between 1.9823(17), 2.0089(18) and 2.0237(9) Å.[27−29] The concomitant lengthening of this P−S bond with the shortening of the external P−C bond suggests there is delocalization within the unsaturated ligand backbone. Theoretical calculations to clarify this point will be presented below. The structure of **6** shows no other particular features.

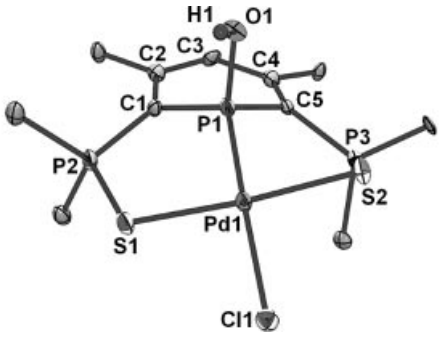

Figure 1. ORTEP view of complex **6**. Atoms are drawn as 50% thermal ellipsoids. Phenyl groups are omitted for clarity. The numbering is arbitrary and different from that used in the NMR spectroscopic data. Selected bond lengths [Å]: P1−C1 1.757(4), C1−C2 1.420(5), C2−C3 1.391(5), C3−C4 1.407(5), C4−C5 1.384(5), C5−P1 1.767(4), P1−O1.597(4), P2−C1, 1.759(4), P2−S1 2.039(2), P3−C5 1.776(4), P3−S2 2.1018(2), P1−Pd1 2.186(1), S1−Pd1 2.310(1), S2−Pd1 2.353(1), Pd1−Cl1 2.405(1); selected bond and dihedral angles [°]: C1−P1−C5 102.7(2), P1−C1−C2 117.5(3), C1−C2−C3 122.2(4), C2−C3−C4 125.2(4), C3−C4−C5 122.6(4), C4−C5−P1 119.3(3), P1−Pd1−Cl1 174.66(4), S1−Pd1−S2 174.67(4), (mean plane C1−C2−C4−C5)−P1 19.0, (mean plane C1−C2−C4−C5)−C3 4.8. Σangles at P1 316.5

It is relatively difficult to propose a definitive mechanism to account for the formation of **6** from **5**. Indeed, ^{31}P NMR monitoring of the reaction revealed only signals corresponding to **5** and **6**. Two possible mechanisms leading to **6** can be proposed, both of which are promoted by the initial displacement of the COD ligand by the two ancillary phosphane sulfide groups to yield an intermediary $PdCl_2$ complex. In the first mechanism, the close proximity of the P−H and Pd−Cl bond leads to dehydrochlorination to yield HCl and a metallated 1,2-dihydrophosphinine oxide; the last step can be regarded as a (1,3) shift of hydrogen from the C2 carbon atom to the P=O bond (Scheme 4). The second mechanism relies on the phosphane oxide−hydroxyphosphane tautomerism. Thus, displacement of one chloride ligand by the phosphorus atom lone pair would yield a cationic complex that could further undergo a dehydrochlorination. Such metal-promoted P=O to POH or P=S to P−SH rearrangements have been used to prepare palladium-phosphinous or palladium phosphinothious acid complexes, and in C−P coupling.[30−32]

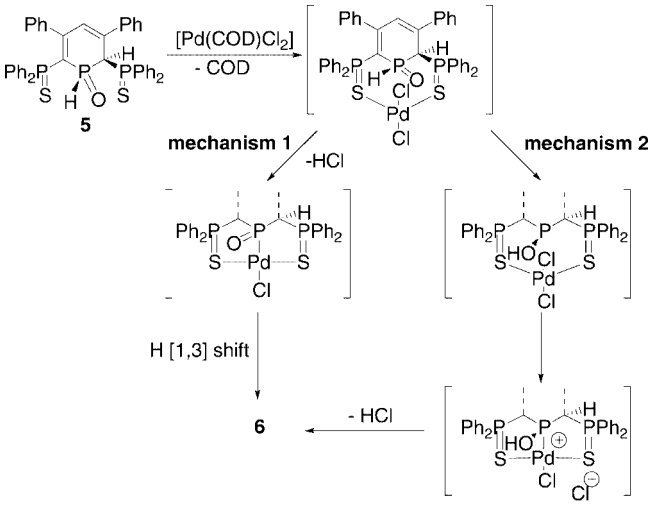

Scheme 4

Compound **1** also reacted with primary alcohols and secondary amines to afford the corresponding λ^5-phosphinines that formally result from the insertion of the phosphorus atom lone pair into the A−H bond (A = RO or R_2N). Whereas the reactions with methanol and ethanol to give **7** and **8** are rather slow and need excess ROH to go to completion, diethylamine readily reacts with **1** to form compound **9**. These derivatives are the first examples of λ^5-phosphinines featuring a P−H bond.[22,33] Both compounds were fully characterized by NMR and mass spectroscopy, as well as by elemental analysis for **7** (Scheme 5). Only primary alcohols react with **1** and additional experiments with menthol and phenol led to the recovery of **1**, even under forcing conditions (heating, high concentration of reagents). In ^{31}P NMR, the formation of **7**, **8**, and **9** was evidenced by the presence of two magnetically equivalent PPh_2S groups. The presence of a P−H bond was definitively established in the ^{1}H NMR spectrum by a strong ^1J(P-H) coupling constant (619.0 Hz in **7**, 613.0 Hz in **8** and 545.0 Hz in **9**).

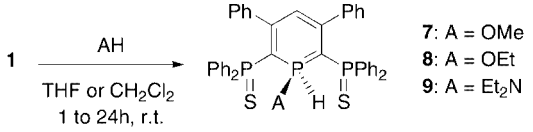

Scheme 5

The formation of λ^5-phosphinines by the direct condensation of alcohols and amines with phosphinines is unprecedented and emphasizes the reactivity of **1**. In most of the several synthetic approaches towards λ^5-phosphinines they are obtained directly by trapping the 1-R-1-*P*-phosphahexadienyl anions with electrophiles. Indeed, these anions are ambident and display two sites of attack, the lone pair at phosphorus and the Cα and Cγ carbon atoms of the carbocyclic backbone. "Soft electrophiles" (MeI for example) react at the phosphorus atom whereas "hard electro-

philes'' (such as H^+) tend to react at the anionic part of the ring to afford 1,2-dihydrophosphinines.[34−36] This is probably why λ^5-phosphinines featuring a PH bond have never been synthesized before (Scheme 6).

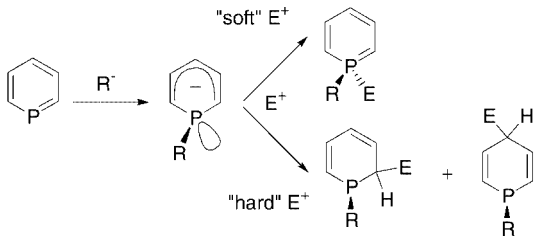

Scheme 6

However, λ^5-phosphinines are supposed intermediates in the thermolysis of 1,2-dihydrophosphinines to produce phosphinines. This transformation, which involves a (1,2) shift of the R group from the Cα carbon atom to phosphorus (Scheme 7) followed by an elimination of AH, usually occurs at high temperature and is well documented.[34,37]

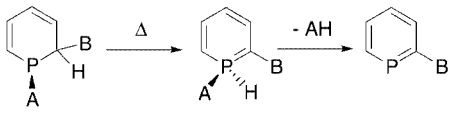

Scheme 7

Though no intermediates could be detected during our experiments, we first supposed that the reaction of MeOH and Et_2NH initially produces transient 1,2-dihydrophosphinines that can further isomerize to yield the corresponding λ^5 derivatives. No theoretical data are available on this isomerization. To clarify this point, DFT calculations were carried out using the combination of the B3LYP functional with the 6-311+G(d,p) basis set. We first focused on the rearrangement of Cα-unsubstituted compounds derived from the parent phosphinine (compounds **Ia**, **b**, **c**, **d**). The relative energies show that the 1,2-dihydro derivative are the most stable isomers (Table 1). Substitution of alkyl groups by OMe or NH_2 groups tends to reduce the energetic difference. This is in good agreement with previous theoretical calculations, which showed that the introduction of an electronegative atom on phosphorus slightly increases the aromaticity of the ring by negative hyperconjugation.[38] However, whatever the substituent at phosphorus, conversions of the 1,2-dihydrophosphinines into the corresponding λ^5-compounds (**IIa**, **b**, **c**, **d**) require a high activation energy (E_A) (from 50.442 kcal/mol for R = OMe to 66.393 kcal/mol for R = H) (Scheme 8). To assess the influence of the substitution pattern of the ring, calculations were performed on a model compound featuring two PPH_2S at the α-positions and a methoxy group at phosphorus. However, as in Cα-unsubstituted derivatives, a high activation barrier (44.848 kcal/mol) is required to form the corresponding λ^5-phosphinine (Scheme 9).

Table 1. Relative energies (ZPE corrected) in kcal/mol of model compounds **I**, **II**, and their corresponding **TS**

I		TS		II	
Ia	0	TSa	+66.393	IIa	+18.235
Ib	0	TSb	+62.475	IIb	+11.790
Ic	0	TSc	+50.442	IIc	+1.892
Id	0	TSd	+57.760	IId	+6.874
Ie	0	TSe	+44.848	IIe	+0.245

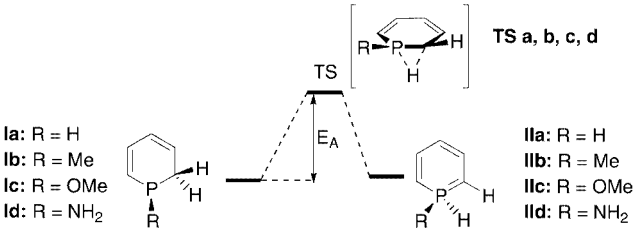

Scheme 8

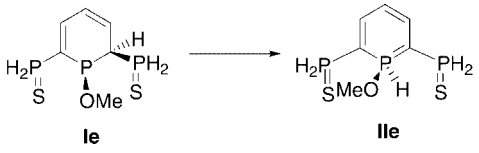

Scheme 9

This short theoretical investigation clearly shows that the introduction of two diphosphanylsulfide groups at the Cα position of phosphorus does not significantly modify the reaction pathway. Therefore, at this stage, no definitive mechanism can be proposed. However, we believe that this transformation is promoted by an initial attack of the oxygen or nitrogen atom at the phosphorus, the two ancillary PPh_2S groups assisting, in a second step, the transfer of H^+ to phosphorus (Scheme 10). Further calculations to localize a possible transition state as well as a complete study on the transformation of λ^5 and dihydrophosphinines into phosphinines are currently underway and will be reported in due course. Very probably, a similar mechanism takes place between **1** and H_2O in the formation of **5** via a transient λ^5-phosphinine. Indeed, λ^5-phosphinines featuring a P−OH group rapidly isomerize to the corresponding 1,2-dihydrophosphinine oxide derivatives.[39]

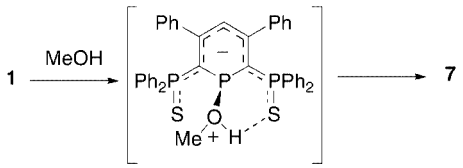

Scheme 10

Interestingly, compounds **7**, **8** can also be used as precursors for the synthesis of P-alkoxy-substituted PdCl complexes. Thus when **7**, **8** were treated with $[Pd(COD)Cl_2]$ in THF at room temperature, complexes **10** and **11** were cle-

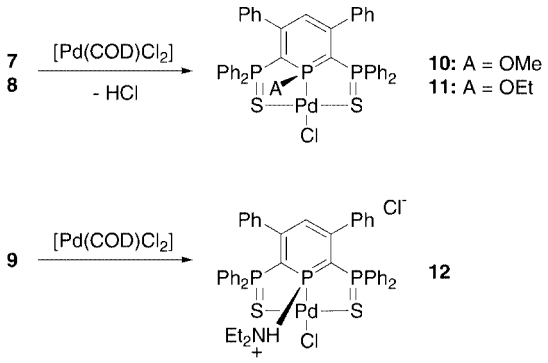

Scheme 11

anly formed in good yields (Scheme 11). Complex **10** has previously been obtained by a nucleophilic substitution of the P−Cl complex. Complex **10** and **11** were identified by NMR techniques and elemental analyses.

The synthesis of an amino derivative proved to be much more difficult to handle because of the concomitant release of HCl. For example, reaction of **9** with $[Pd(COD)Cl_2]$ in THF at room temperature afforded the poorly soluble salt **12**. The formulation of **12** was established on the basis of its ^1H NMR spectrum, which reveals an acidic proton at $\delta(CD_3COCD_3) = 9.25$ ppm, and elemental analyses. The formation of **12** could not be prevented even in the presence of a large excess of diethylamine as HCl scavenger.

Since no intermediates could be detected in ^{31}P NMR spectroscopy during the synthesis of **10** and **11**, no definitive mechanism can be proposed. However, a mechanism close to that proposed for the synthesis of complex **6** seems plausible. In a first step, the COD ligand is displaced from palladium by the two ancillary sulfide ligands and an elimination of HCl takes place to form the P−Pd bond (Scheme 12).

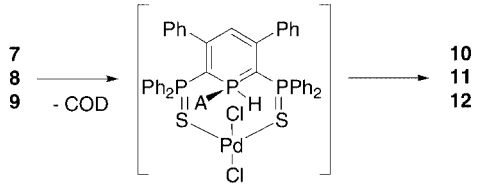

Scheme 12

Alkoxy complexes can also be obtained by the classical route that relies on the displacement of the Cl atom from phosphorus by ROH in complex **2**. Thus, complex **13** was easily obtained by treating (−)-menthol with **2** in dichloromethane at room temperature. The formation of **13** was evidenced by an ABC spin system pattern in ^{31}P NMR spectrum − a result of the chiral group introduced at phosphorus, which renders the two ancillary PPh_2S substituents magnetically non-equivalent (see Exp. Sect.). The formulation of **13** was confirmed by an X-ray structural study. A view of one molecule of **13** and the most significant metric

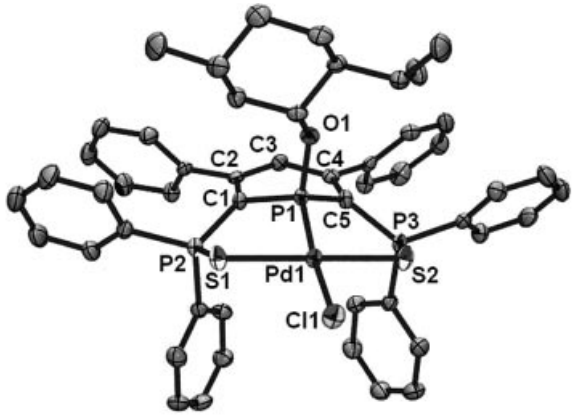

Figure 2. ORTEP view of complex **13**. Atoms are drawn as 50% thermal ellipsoids. The numbering is arbitrary and different from that used in the NMR spectroscopic data; selected bond lengths [Å]: P1−C1 1.761(3), C1−C2 1.408(4), C2−C3 1.389(4), C3−C4 1.409(4), C4−C5 1.407(4), C5−P1 1.751(3), P1−Pd1 2.188(1), C1−P2 1.778(3), P2−S1 2.033(2), C5−P3 1.774(3), P3−S2 2.033(2), P1−O1 1.600(2), S1−Pd1 2.328(1), S2−Pd1 2.313(1), Pd1−Cl1 2.396(1). Selected angles and dihedral angles [°]: P1−C1−C2 118.2(2), C1−C2−C3 122.0(3), C2−C3−C4 125.7(3), C3−C4−C5 121.2(3), C4−C5−P1 118.6(2), P1−Pd1−Cl1 170.11(3), S1−Pd1−S2 172.98(3). C4−C2−C1−P1 20.0, C1−C5−C4−C3 5.2, (mean plane C1−C2−C4−C5)−P1 20.9, (mean plane C1−C2−C4−C5)−C3 5.5. Σangles at P1 313.3

parameters (Figure 2), and crystal data and structural refinement details (Table 6), are given. This route was also efficient for the synthesis of the amino derivative **14**. Reaction of Et_2NLi with **2** in THF at low temperature cleanly afforded **14** which was recovered as a yellow solid in nearly quantitative yield (Scheme 13).

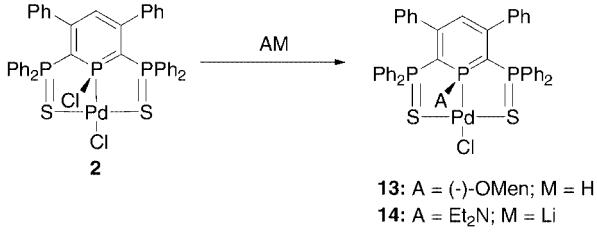

Scheme 13

The structure of **14** was confirmed by an X-ray analysis. An ORTEP view of one molecule of **14** (Figure 3), and crystal data and structural refinement details (Table 7), are given. The structure of **14** does not significantly differ from that of **5**. The two internal P−C bond lengths [P1−C1 1.756(2) Å and P1−C5 1.763(2) Å] as well as the external ones [C1−P2 1.766(2) Å and C5−P3 1.762(2) Å] are also short, and the two P−S bond lengths [P2−S1 2.029(1) Å and P3−S2 2.033(1) Å] are long.

Our investigations on potential precursors of these palladium(II) complexes have yielded another approach to P-alkyl derivatives. Reaction of anion **15** with C_2Cl_6 afforded the λ^5-phosphinine **16** featuring a P−Cl bond (Scheme 14). This compound, isolated as a moisture-sensitive solid, was successfully characterized by NMR and mass spectroscopy.

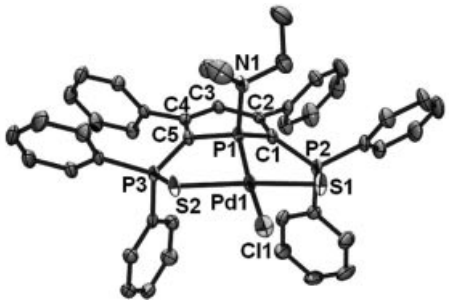

Figure 3. ORTEP view of complex **14**. Atoms are drawn as 50% thermal ellipsoids. The numbering is arbitrary and different from that used in the NMR spectroscopic data; selected bond lengths [Å]: P1−C1 1.756(2), C1−C2 1.409(3), C2−C3 1.408(3), C3−C4 1.400(3), C4−C5 1.411(3), C5−P1 1.763(2), P1−N1 1.681(2), P2−C1 1.766(2), P2−S1 2.029(1), C5−P3 1.762(2), P3−S2 2.033(1), P1−Pd1 2.186(1), S1−Pd 2.3250(8), S2−Pd 2.3275(8), Pd1−Cl1 2.404(1). Selected angles and dihedral angles [°]: C1−P1−C5 103.3(1), P1−C1−C2 117.0(2), C1−C2−C3 122.3(2), C2−C3−C4 125.3(2), C3−C4−C5 122.2(2), C4−C5−P1 117.3(2), P1−Pd1−Cl1 167.07(2), S1−Pd−S2 171.42(2), (mean plane C1−C2−C4−C5)−P1 20.6, (mean plane C1−C2−C4−C5)−C3 5.75. Σangles at P1 314.1

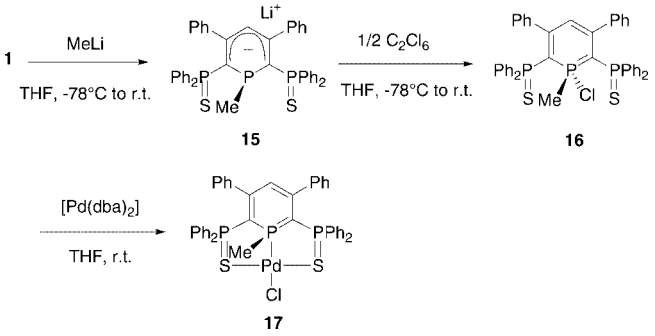

Scheme 14

Interestingly, **16** reacts with the [Pd(dba)$_2$] complex to form complex **17** (Scheme 14), which can be rationalized following a classical mechanism that involves the insertion of palladium into the P−Cl bond of **16**. Practically, this route is probably less straightforward than the direct reaction of anion **15** with [Pd(COD)Cl$_2$]. (Scheme 1) However, it shows that zerovalent metal centers can readily be inserted into the P−Cl bond of λ^5-phosphinines. This strategy could be particularly useful when divalent metal precursors are not available.

We wished to extend our several methods devised to introduce any substituent at the phosphorus to nickel and platinum(II) derivatives. All the approaches developed with palladium complexes have not yet been systematically explored. The original method involving the displacement of a chloride atom from the metal to the phosphorus atom could be duplicated with nickel and platinum using [NiBr$_2$(DME)] (DME = dimethoxyethane) and [Pt(COD)Cl$_2$] as starting precursors. Both reactions took place in dichloromethane at room temperature to afford

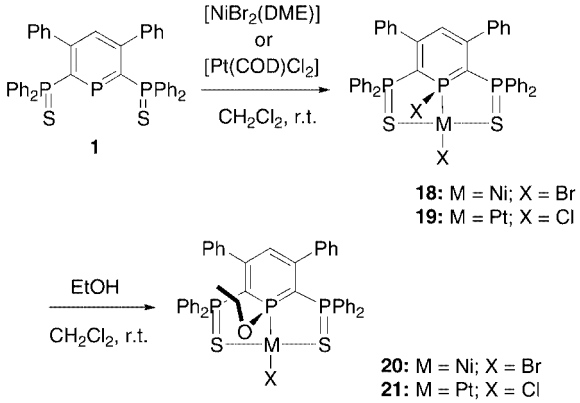

Scheme 15

complexes **18** and **19** respectively (Scheme 15). The P−Br **18** and P−Cl **19** derivatives, which are moisture sensitive, were characterized by ^{31}P NMR spectroscopy and by X-ray diffraction studies. However their structures, which are similar to that of the Pd−Cl complex **2**, are not reported here. As with the palladium derivative the P−Br and P−Cl bonds are sufficiently reactive to undergo nucleophilic substitution. Thus, reaction of EtOH with **18** and **19** cleanly afforded complexes **20** and **21**, respectively, which were fully characterized by NMR and mass spectroscopy as well by elemental analysis. Under standard conditions, intermediates **18** and **19** need not be isolated (Scheme 15).

Nickel and platinum complexes of alkyl derivatives were also prepared using the anionic approach. Phosphinine **1** reacted with *n*BuLi in THF at low temperature to produce anion **3** which was subsequently treated with [NiBr$_2$(DME)] and [Pt(COD)Cl$_2$] to yield complexes **22** and **23**, respectively (Scheme 16). The NMR spectroscopic data of **22** and **23** are comparable to those of their palladium analog **4**.

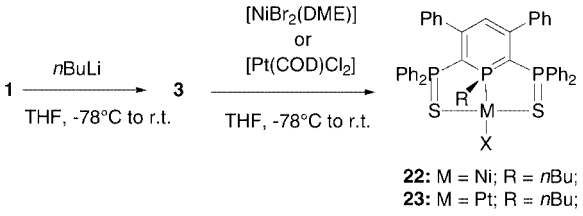

Scheme 16

Complex **22** was structurally characterized. An ORTEP view of one molecule of **22** and the most significant metric parameters (Figure 4), and crystal data and structural refinement details (Table 7), are presented here. These data reveal that replacement of palladium by nickel does not significantly modify the λ^5-phosphinine backbone, and the same trends are observed. The P−C bonds (external and internal) are short and the P−S bonds are slightly lengthened. The two angles between the C1−C2−C4−C5 plane and the phosphorus atom (21.05°) and the C3 carbon (4.7°)

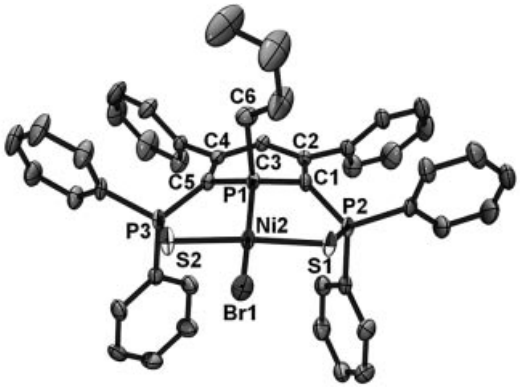

Figure 4. ORTEP view of complex **22**. Atoms are drawn as 50% thermal ellipsoids. The numbering is arbitrary and different from that used in the NMR spectroscopic data; selected bond lengths [Å]: P1−C1 1.776(3), C1−C2 1.384(5), C2−C3 1.412(4), C3−C4 1.412(4), C4−C5 1.390(5), C5−P1 1.778(3), P1−Ni2 2.111(1), C1−P2 1.768(3), P1−C6 1.829(4), P2−S1 2.039(2), C5−P3 1.761(3), P3−S2 2.045(2), P1−C6 1.829(4), S1−Ni2 2.185(1), S2−Ni2 2.194(1), Ni2−Br1 2.363(1). Selected angles [°]: P1−C1−C2 129.4(2), C1−C2−C3 121.8(3), C2−C3−C4 124.9(3), C3−C4−C5 122.8(3), C4−C5−P1 118.0(2), P1−Ni2−Br1 163.89(3), S1−Ni2−S2 172.57(4). (mean plane C1−C2−C4−C5)−P1 21.05, (mean plane C1−C2−C4−C5)−C3 4.7. Σangles at P1 315.3

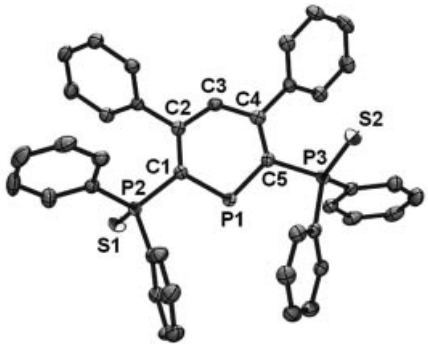

Figure 5. ORTEP view of phosphinine **1**. Ellipsoids are 50% thermal ellipsoids. The numbering is arbitrary and different from that used in the NMR spectroscopic data; selected bond lengths [Å]: P1−C1 1.742(2), P1−C5 1.745(2), C1−C2 1.409(3), C2−C3 1.399(3), C3−C4 1.399(3), C4−C5 1.417(3), P2−C1 1.826(2), S1−P2 1.956(1), P3−C5 1.835(2), S2−P3 1.9532(8). Selected angles [°]: C1−P1−C5 103.9(1), P1−C1−C2 123.2(2), C1−C2−C3 121.0(2), C2−C3−C4 127.9(2), C3−C4−C5 120.4(2), C4−C5−P1 123.3(2), P1−C1−P2 111.8(1), P1−C5−P3 112.9(1), C1−P2−S1 112.73(7), C5−P3−S2 112.54(8), (mean plane C1−C2−C4−C5)−P1 4.1, (mean plane C1−C2−C4−C5)−C3 3.7

atom also compare with those of **5**, **13** and **14** as well as the pyramidality of the phosphorus atom.

Finally, a preliminary study of the reactivity of the halogen ligand in these complexes showed that the chloride (Pd and Pt) or bromide ligand (Ni) is easily abstracted upon reaction with $AgBF_4$ in dichloromethane at room temperature in the presence of acetonitrile (Scheme 17). Four cationic complexes **24**−**27** were thus obtained and fully characterized by NMR techniques and elemental analyses. Interestingly, reaction of the palladium complex **4** with AgOTf furnished the neutral complex **28**. Its formulation was unambiguously established on the basis of NMR spectroscopic data and elemental analysis.

Having developed several new synthetic pathways to these d^8 metal complexes, we turned our attention to the electronic structure of the SPS pincer ligands. As noted earlier, some X-ray structural data suggest that electronic delocalization occurs within the ligand. To establish a significant structural comparison, three compounds were crystallized and submitted to X-ray crystal structure analysis, the phosphinine precursor **1**, the free anionic ligand **15** and the λ^5-dimethylphosphinine **29**. Phosphinine **1** was easily crystallized by diffusion of hexanes into a solution of **1** in CH_2Cl_2. An ORTEP view of one molecule of **1** and the most relevant metric parameters (Figure 5), and crystal data and structural refinement details (Table 5), are presented.

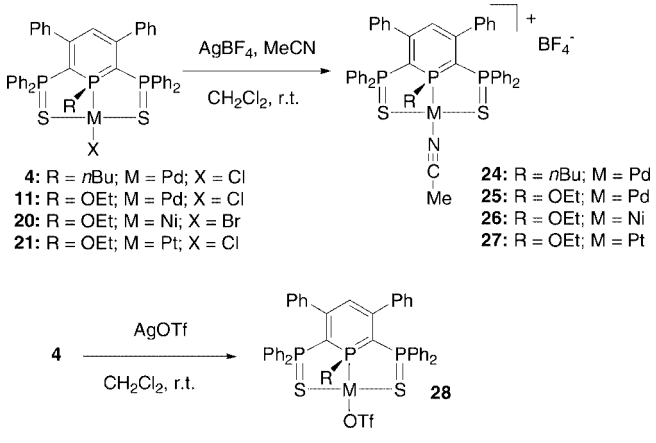

Scheme 17

Compound **29** was prepared conventionally with the subsequent trapping of anion **15** with methyl iodide. As explained above, in good agreement with literature data, the alkylation takes place exclusively at the phosphorus atom lone pair to yield **29** in very good yields (Scheme 18). The formulation of **29** was easily established on the basis of NMR spectroscopic data and combustion analysis. Suitable crystals were obtained by diffusion of hexanes into a solution of **29** in $CDCl_3$. An ORTEP view of one molecule of **29** and the most significant metric parameters (Figure 6), and crystal data and structural refinement details (Table 5), are given.

The crystallization of an anionic derivative of **1** proved to be much more difficult. To draw a precise comparison with the dimethyl-λ^5-phosphinine **29**, the crystallization of anion **15** was attempted. However, whatever the experimental conditions used (solvent, temperature, presence or absence of cryptand) no suitable crystals could be grown. However, crystallization of the methoxy-substituted species **30** gave more satisfying results. Anion **30** was readily prepared by reacting 3 equivalents of MeONa with **1** in THF at room temperature (Scheme 19). Suitable crystals of this anion were obtained upon crystallization with the (2.2.2) cryptand. An ORTEP view of one molecule of **30** and the most relevant bond lengths and bond angles (Figure 7), and crystal data and structural refinement details (Table 5), are presented.

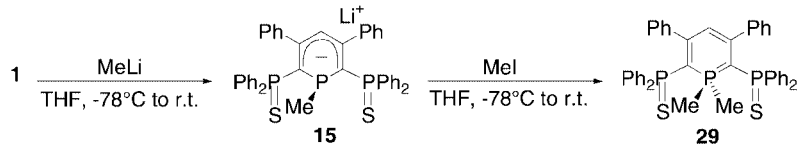

Scheme 18

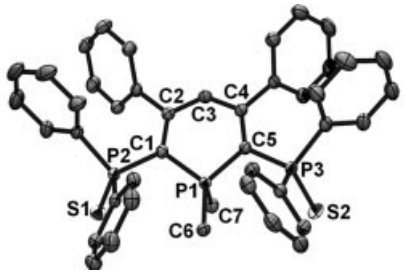

Figure 6. ORTEP view of phosphinine **29**. Ellipsoids are 50% thermal ellipsoids. The numbering is arbitrary and different from that used in the NMR spectroscopic data; selected bond lengths [Å]: P1−C1 1.767(2), P1−C5 1.768(2), C1−C2 1.410(2), 1.410(2), C2−C3 1.402(2), C3−C4 1.411(2), C4−C5 1.404(2), P1−C6 1.799(2), P2−C1 1.789(2), S1−P2 1.9675(8). Selected angles [°]: C1−P1−C5 106.25(8), P1−C1−C2 112.3(1), C1−C2−C3 123.1(2), C2−C3−C4 126.6(2), C3−C4−C5 122.7(2), C4−C5−P1 113.0(1), P1−C1−P2 120.9(1), P1−C5−P3 119.2(1), C1−P2−S1 114.24(7), C4−P3−S2 113.36(7), (mean plane C1−C2−C4−C5)−P1 37.0, (mean plane C1−C2−C4−C5)−C3 17.0

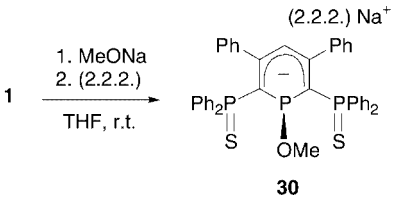

Scheme 19

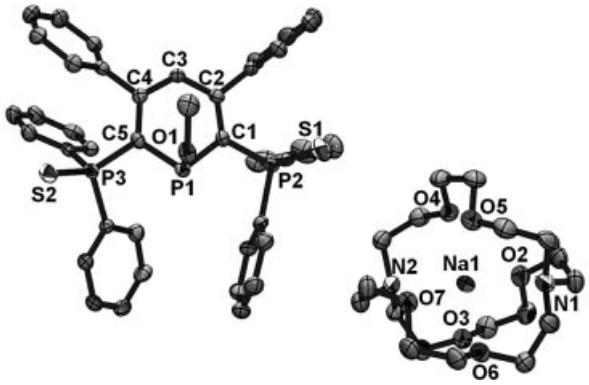

Figure 7. ORTEP view of anion **30**. Ellipsoids are 50% thermal ellipsoids. The numbering is arbitrary and different from that used in the NMR spectroscopic data; selected bond lengths [Å]: P1−C1 1.802(4), C1−C2 1.390(7), C2−C3 1.408(7), C3−C4 1.393(6), C5−C5 1.406(7), C5−P1 1.791(5), C5−P1 1.791(5), C1−P2 1.794(5), C5−P3 1.770(4), P3−S2 1.974(2), P2−S1 1.968(2), P1−O1 1.661(4). Selected angles and dihedral angles [°]: C5−P1−C1 105.0(2), P1−C1−C2 121.5(3), C1−C2−C3 122.6(4), C2−C3−C4 125.4(4), C3−C4−C5 121.4(4), C4−C5−P1 122.2(3), P1−C5−P3 116.4(3), P1−C1−P2 115.9(3), (mean plane C1−C2−C4−C5)−P1 21.0, (mean plane C1−C2−C4−C5)−C3 6.0

The structural data of **1**, **29**, and **30** provide interesting information. The structure of ligand **1** is relatively classical and compares with those of other λ^3-phosphinines. The two internal P=C bond lengths and the C−C bond lengths within the ring fall in the usual range and the ring is planar. The two sulfide groups point towards the back of the molecule to minimize the electronic repulsion between the lone pair at phosphorus and that of sulfur atoms (Figure 5). Of most interest is the external P−C bond lengths [C1−P2 1.826(2) Å and C5−P3 1.835(2) Å], which compare with those of classical P−C single bonds. Moreover, the P=S bond lengths [P2−S1 1.956(1) Å and P3−S2 1.953(1) Å] are normal. Transformation of **1** into **29** obviously induces important distortions and the phosphorus atom now escapes, by 23.15°, from the C1−C2−C4 and C5 plane. While the ylidic structure of the ring is evidenced by a small lengthening of the internal P−C bonds, the two external ones are slightly shortened [1.789(2) Å and 1.792(2) Å], suggesting that a delocalization occurs. However, this delocalization is probably weak and does not extend to the two P=S bonds due to the orientation of the two phosphane-sulfides groups, which are not coplanar with the unsaturated part of the ring. This effect is also apparent in **30**, which consists of two discrete units of the anionic ligand and [Na(2.2.2)]. Though the substituent at phosphorus is different (Me in **29**, OMe in **30**), the introduction of the charge significantly modifies the hybridization state of the phosphorus atom. Thus, in **30** the two internal P−C bond lengths [1.802(4) Å and 1.791(5) Å] have lost their ylidic character and this anion can be considered as a simple phosphanyl-substituted pentadienyl anion.[40] Note also that, as in **29**, the two external P−C bond lengths [1.794(5) Å and 1.770(4) Å] are also quite short.

These data do not obviously compare with those of the Pd and Ni complexes, and it is relatively difficult to establish whether the ligand behaves as an anionic λ^4-phosphinine (form A) or as a classical tertiary phosphane (form B). The short internal P−C bond lengths suggest that the ylidic structure of the phosphinine has been restored upon complexation but, conversely, the relatively long P−S bonds and short external P−C connections point to delocalization within the unsaturated part of the ligand (form B) (Scheme 20).

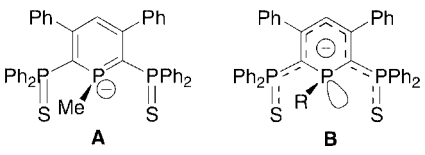

Scheme 20

Reasonably, one may propose that both forms can contribute to the bonding, the respective contributions being determined by the nature of the metal centre and its formal oxidation state. Lacking a wide range of complexes and X-ray structures, it seems premature to propose a definitive model to rationalize the bonding in these complexes. A preliminary theoretical study aimed at evaluating the electronic capacity of the ligand in these group 10 complexes was thus undertaken. Optimizations were carried out on the two model complexes **IIIa**, **b** featuring a methyl group and a methoxy group at phosphorus, respectively (Scheme 21). The ligand substitution scheme was simplified to save computation time, and phenyl groups of the phosphane sulfide substituents, as well as those located on the phosphinine ring, were replaced by hydrogen atoms (Scheme 21).

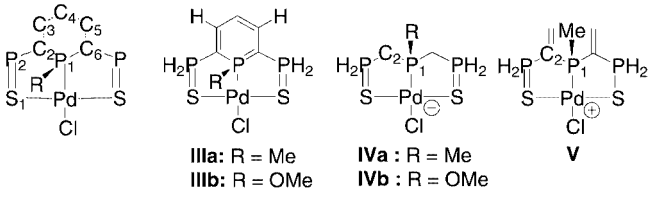

Scheme 21

Various functional and basis sets were tested. The best compromise, in terms of computation time and accuracy of structural data, was a combination of the B3LYP functional with a mixed basis set composed of the 6-31G* basis set for C, H, O, P, S and Cl atoms and the effective core potentials (ECP) of Hay and Wadt for Pd. The most significant bond lengths and bond angles of **IIIa**, **b** (Table 2) show an acceptable fit between theoretical and experimental parameters. Thus, the same trend is seen for P−C (internal and external) and P−S bond lengths. For example in **IIIa**, the internal P−C bonds (1.796 Å) are close to that in the *n*Bu derivative [1.762(7) Å] whose structure was previously reported. In **IIIb**, the external P−C bonds are shortened (1.774 Å *vs* 1.778(3) Å in **13**) and the P−S bonds are lengthened (2.049 Å vs. 2.033(2) Å in **13**). The only discrepancies arise from the P−Pd and S−Pd bond lengths and from the dihedral angle measuring the out-of-plane distortion of the phosphorus atom. Indeed, P−Pd and S−Pd bond lengths are overestimated and the out-of-plane distortion is underestimated in the theoretical structures. However, modification of the basis set for Pd (all electron-basis sets, other ECP, diffuse functions) or phosphorus and sulfur (diffuse functions) did not significantly improve data.

An analysis of natural charge (NBO method) reveals that, in **IIIa**, **b**, the phosphorus atom bears a significant positive charge and that the α (C2 and C6) and γ (C4) carbon atoms are negatively charged (Table 3). Conversely, the β (C3 and C5) carbon atoms are positively charged. This charge distribution is relatively equivalent to that observed in λ^5-phosphinines (see for example data for **IIe**). However, a relatively similar charge distribution is observed in the phosphane-based complexes **IVa**, **b** and **V**. These data also suggest that the P−Pd bond is slightly more polarized in **IIIa**, **b** than in **IVa**, **b** and **V**, but these differences are not very significant. Care must be taken in drawing rapid conclusion from charge distributions, especially in transition metal complexes.

Table 2. Most significant geometrical data for calculated structures **IIIa**, **b**, **IVa**, **b**, and **V**. Distances [Å] and angles [°]

	IIIa	IIIb	IVa	IVb	V
P1−C2	1.796	1.780	1.881	1.882	1.843
C2−C3	1.395	1.397			
C3−C4	1.404	1.403			
C2-P2	1.768	1.774	1.856	1.859	1.829
P2−S1	2.050	2.049			
P1−R	1.846	1.650	1.834	1.612	1.836
P1−Pd	2.258	2.243	2.300	2.275	2.302
Pd1−Cl	2.377	2.377	2.322	2.323	2.324
C6−P1−C2	101.7	101.5	107.4	106.6	108.0

Table 3. Calculated NBO charge distribution for ligands **IIe**, **f**, and complexes **IIIa**, **b** and **V**

	IIe	IIIa	IIIb	IVa	IVb	V
P1	1.662	1.170	1.420	1.038	1.375	1.060
C2	−0.950	−0.922	−0.942	−1.123	−1.156	−0.744
C3	−0.136	−0.139	−0.151			
C4	−0.326	−0.350	−0.334			
P2	0.880	0.921	0.917	0.850	0.846	0.856
S	−0.563	−0.457	−0.398	−0.302	−0.293	−0.308
Pd		0.351	0.367	0.313	0.310	0.323
Cl		−0.576	−0.560	−0.433	−0.437	−0.440

To determine which form (A or B) is preponderant in the bonding to the metal, a charge decomposition analysis was carried out using the CDA program developed by Frenking and coll. Such analysis has proved to be very useful in estimating the ratio between donation and back-donation for ligands following the classical Dewar−Chatt−Duncansson (DCD) model. Further explanations about the method, the terms used in these calculations and their relevance are given in the theoretical section. Complexes **IIIa**, **b** were compared to the virtual cationic complexes **IVa**, **b**, and **V** featuring a tertiary phosphane as central ligand and two peripheral phosphane sulfide groups. Complex **V** only differs from **IVa** by the presence of two exocyclic CH_2 groups which mimic the unsaturated backbone of the phosphinine ring.

The results of the CDA analysis are presented in Table 4. A first important remark concerns the residual term (Δ) which allows one to consider the interaction in terms of donor−acceptor behavior. All of the complexes exhibit a low (Δ) value, indicating that their bonding to Pd can be described following the DCD model. The second interesting point concerns the $b/(d+b)$ value which reflects the percentage of π-acceptance. The similarity of these values clearly indicates that the central phosphorus atom in **IIIa**, **b** (15.19 and 19.23%) exhibits electronic properties that are close to

Table 4. Charge decomposition analysis of complexes **IIIa**, **b**, **IVa**, **b**, and **V**

	IIIa	IIIb	IVa	IVb	V
d[a]	1.089	0.844	0.855	0.935	0.863
b[b]	0.195	0.201	0.171	0.160	0.147
d/b	5.58	4.20	5.00	5.843	5.87
$b/(d+b)$	15.19	19.23	16.66	14.62	14.55
r[c]	−0.397	−0.076	0.069	−0.092	−0.093
Δ	−0.008	−0.005	−0.001	0.025	0.004

those of classical tertiary phosphane complexes **IV** and **V** (between 14.55 and 16.66%). Note that the exocyclic double bonds in **V** do not significantly modify the electronic capacity of the ligand. Overall, we therefore propose that, at least in the case of d^8 palladium complexes, the delocalized form B is probably preponderant.

Conclusion

We have presented several unusual routes towards λ^5-phosphinines derivatives of the 2,6-bis(diphenylphosphanyl)phosphinine. Easy access towards previously unknown P−H derivatives and a straightforward preparation of a P−Cl derivative have also been devised. Additionally, new synthetic approaches towards SPS-λ^5 phosphinine group 10 metal complexes have been developed using either these P−H, P−Cl derivatives or a 1,2-dihydrophosphinine oxide. Most of these routes should be operative with other metal halides. Structural data as well as a preliminary theoretical investigation suggests that a delocalization takes place within the carbocyclic part of the ligand but that the central phosphorus atom behaves as a classical tertiary phosphane. Further studies will now focus on the catalytic properties of the group 10 complexes and on a systematic investigation of the coordinative properties of SPS based-ligands. A detailed theoretical study of their electronic properties will be reported elsewhere.

Experimental Section

General Remarks: All reactions were routinely performed under an inert atmosphere of argon or nitrogen using Schlenk and glove-box techniques and dry deoxygenated solvents. Dry THF and hexanes were obtained by distillation from Na/benzophenone and dry diethyl ether from $CaCl_2$ and then NaH and dry CH_2Cl_2 from P_2O_5. Acetonitrile (99.5% purity) was purchased from SDS and used without further purification. $CDCl_3$ was dried over P_2O_5, and stored on 4Å Linde molecular sieves. CD_2Cl_2, [D_8]THF, and [D_6]acetone were used as purchased and stored in the glove-box. Nuclear magnetic resonance spectra were recorded on a Bruker AC-200 SY spectrometer operating at 300.0 MHz for ^{1}H, 75.5 MHz for ^{13}C and 121.5 MHz for ^{31}P. Solvent peaks were used as internal reference relative to Me_4Si for ^{1}H and ^{13}C chemical shifts (ppm); ^{31}P chemical shifts are relative to an 85% H_3PO_4 external reference. Coupling constants are given in Hertz. The following abbreviations are used: s, singlet; d, doublet; t, triplet; q, quadruplet; p, pentuplet; m, multiplet; v, virtual; b, broad. Mass spectra were obtained at 70 eV with a HP 5989B spectrometer coupled to a HP 5980 chromatograph by the direct inlet method. Elemental analyses were performed by the "Service d′analyse du CNRS", at Gif sur Yvette, France. Phosphinine **1** and complex **2**,[21] anion **3** and complex **4**,[22] [Ni(dme)Br_2],[41] [Pd(COD)Cl_2],[42] [Pd(dba)$_2$],[43] and [Pt(COD)Cl_2][44] were prepared according to reported procedures.

Phosphinine 1: Suitable crystals for X-ray structure analysis were grown by diffusion of hexanes into a solution of **1** in CH_2Cl_2.

Phosphane Oxide 5: Water (0.1 ml) was added to a solution of **1** (370 mg, 0.54 mmol) in THF (20 mL). The reaction was then stirred for 5 min at room temperature and the solvent was removed under vacuum. The solid was washed with diethyl ether (2 × 5 mL) and, after drying, **5** was recovered as a yellow powder. Suitable crystals for X-ray structure analysis were grown from a diffusion of hexanes into a solution of **5** in CH_2Cl_2.Yield: 97%, 366 mg. ^{1}H NMR (300 MHz, $CDCl_3$, 298 K): δ = 5.05 [ABB′X, td, ^2J(H-P_A) = ^2J(H-P_B) = 16.6, ^3J(H−H) = 2.1, 1 H, H^2], 6.55 (ABB′X, m, ΣJ= 9, 1 H, H^4), 6.74 [dd, ^1J(H-P_A) = 580, ^3J(H−H) = 2.7, 1 H, PH], 6.82−8.20 (m, 30 H, CH of Ph) ppm. ^{13}C NMR (75.5 MHz, $CDCl_3$, 298 K): δ = 43.5 (m, C^2H), 119.9 (m, C^6), 127.7−133.4 (m, C^4H, CH and C of Ph), 137.4 (ABB′X, m, ΣJ= 20, $C^{5\ or\ 3}$), 140.5 (ABB′X, m, ΣJ= 21, $C^{3\ or\ 5}$), 163.4 [d, ^3J(C-P_A) = 3.7, C of Ph] ppm. ^{31}P NMR (121.5 MHz, $CDCl_3$, 298 K): δ = 4.22 [ABB′, dd, ^2J(P_A-P_B) = 35.3, ^2J(P_A-$P_{B'}$) = 17.0, P_AH], 36.47 [ABB′, d, ^2J(P_A-P_B) = 35.3, P_BPh$_2$], 38.92 [ABB′, d, ^2J(P_A-$P_{B'}$) = 17.0, $P_{B'}$Ph$_2$] ppm. MS (EI): m/z = 682 [M^+ − (H_2O)]. $C_{41}H_{33}OP_3S_2$ (698.75): calcd. C 70.47, H 4.76; found C 70.03, H 4.34.

Complex 6: A solution of [Pd(COD)Cl_2] (155 mg, 0.54 mmol) and **5** (380 mg, 0.54 mmol) in CH_2Cl_2 (10 mL) was stirred for 2 h at room temperature. After removing the solvent under vacuum, the resultant yellow solid was washed with hexanes (3 × 5 mL) and dried. Suitable crystals for an X-ray structure analysis were grown from a diffusion of hexanes into a solution of $CDCl_3$. Yield: 83%, 376 mg. ^{1}H NMR (300 MHz, $CDCl_3$, 298 K): δ = 5.83 (m, 1 H, H^4), 6.60−7.60 (m, 30 H, CH of Ph) ppm. ^{31}P NMR (121.5 MHz, $CDCl_3$, 298 K): δ = 54.36 [AB_2, d, ^2J(P_A-P_B) = 105.7, P_BPh$_2$], 90.10 [AB_2, t, ^2J(P_A-P_B) = 105.7, P_A] ppm. Complex **6** was too insoluble to a give a satisfactory ^{13}C NMR spectrum. $C_{41}H_{32}ClOP_3PdS_2$ (839.62): calcd. C 58.65, H 3.84; found C 58.28, H 3.47.

λ^5-Phosphinine 7: A solution of **1** (100 mg, 0.15 mmol) and methanol (200 μL, 4.9 mmol) in THF (5 mL) was stirred for 24 h at 40 °C. After removing the solvent under vacuum, the resultant yellow solid was washed first with hexanes (3 × 2 mL) and then with diethyl ether (3 × 2 mL). After drying, **7** was recovered as a yellow powder in 73% (78 mg) yield. ^{1}H NMR (300 MHz, CD_2Cl_2, 298 K): δ = 3.38 (d, $^3J_{H-P}$ = 13.8, 3 H, CH_3), 5.7 [td, ^4J(H-P_B) = 3.8, ^4J(H-P_A) = 1.7, 1 H, H^4], 7.56 [dt, ^1J(H-P_A) = 619.0, ^3J(H-P_B) = 1.9, 1 H, PH], 6.80−7.76 (m, 30 H, CH of Ph) ppm. ^{13}C NMR (75.5 MHz, CD_2Cl_2, 298 K): δ = 49.5 (br. s, CH_3), 80.7 (m, $C^{2,6}$), 116.3 (m, C^4H), 125.8−133.5 (m, CH and C of Ph), 140.5 [m, ΣJ(C-P) = 20.7, $C^{3,5}$], 156.4 (s, C of Ph) ppm. ^{31}P NMR (121.5 MHz, CD_2Cl_2, 298 K): δ = 27.57 [AB_2, t, ^2J(P_A-P_B) = 43.7, P_A], 39.46 [AB_2, d, ^2J(P_A-P_B) = 43.7, P_B] ppm. MS (EI): m/z = 682 [M^+ − (MeOH)]. $C_{42}H_{35}OP_3S_2$ (712.78): calcd. C 70.77, H 4.95; found C 70.31, H 4.44.

λ^5-Phosphinine 8: A solution of **1** (550 mg, 0.8 mmol) and ethanol (200 μL, 3.4 mmol) in THF (5 mL) was stirred for 24 h at 40 °C. After removing the solvent under vacuum, the resultant solid was

washed first with hexanes (3 × 2 mL) and then with diethyl ether (3 × 2 mL). After drying, **8** was recovered as a yellow powder in 78% (433 mg) yield. ^{1}H NMR (300 MHz, CD_2Cl_2, 298 K): δ = 1.26 [t, ^3J(H−H) = 7.2, 3 H, CH_3], 3.90 [dq, ^3J(H−H) = ^3J(H-P_A) = 7.2, 2 H, CH_2], 5.72 [t, ^4J(H-P_B) = 7.2, 1 H, H^4], 6.84−7.76 (m, 30 H, CH of Ph), 7.73 [d, ^1J(H-P_A) = 613.0, 1 H, PH] ppm. ^{13}C NMR (75.5 MHz, CD_2Cl_2, 298 K): δ = 15.1 [d, ^3J(C-P_A) = 16.0, CH_3], 63.3 [d, ^2J(C-P_A) = 6.9, CH_2O], 81.7 [ddd, ^1J(C-P_A) = 101.2, ^1J(C-P_B) = 80.5, ^3J(C-$P_{B'}$) = 4.6, $C^{2,6}$], 117.2 (m, C^4H), 127.1−132.2 (m, CH of Ph), 133.5 [dd, ^1J(C-P_B) = 11.5, ^3J(C-P_A) = 3.5, C of Ph], 134.7 [dd, ^1J(C-P_B) = 13.8, ^3J(C-P_A) = 3.4, of Ph], 141.5 [dt, ^2J(C-P_A) = 11.5, ^2J(C-P_B) = ^4J(C-$P_{B'}$) = 3.4, $C^{3,5}$], 156.3 (s, C of Ph) ppm. ^{31}P NMR (121.5 MHz, CD_2Cl_2, 298 K): δ = 25.87 [AB_2X, t, ^2J(P_A-P_B) = 43.1, P_A], 39.46 [AB_2, d, ^2J(P_A-P_B) = 43.1, P_B] ppm. MS (EI): *m*/*z* = 682 [M^+ − (EtOH)]. $C_{43}H_{37}OP_3S_2$ (726.81): calcd. C 71.06, H 5.13; found C 70.67, H 4.82.

λ^5-Phosphinine 9: A solution of **1** (100 mg, 0.15 mmol) and diethylamine (200 μL, 1.9 mmol) in CH_2Cl_2 (5 mL) was stirred for 15 min at room temperature. After removing the solvent under vacuum, the so-obtained yellow solid was washed first with hexanes (3 × 2 mL) and then with diethyl ether (3 × 2 mL). After drying, **9** (98 mg) was recovered as a yellow powder in 87% yield. ^{1}H NMR (300 MHz, $CDCl_3$, 298 K): δ = 1.14 [t, ^3J(H−H) = 6.9, 6 H, CH_3], 2.92 [q, ^3J(H−H) = 6.9, 4 H, CH_2], 5.59 [t, ^3J(H-P_B) = 4.6, 1 H, H^4], 7.29 [dt, ^1J(H-P_A) = 545.0, ^1J(H-P_B) = 2.0, 1 H, PH], 6.76−7.72 (m, 30 H, CH of Ph) ppm. ^{13}C NMR (75.5 MHz, $CDCl_3$, 298 K): δ = 10.9 (s, CH_3), 41.5 [d, ^2J(C-P_A) = 19.6, CH_2], 87.6 (m, $C^{2,6}$), 113.9 [d, ^4J(C-P_A) = 13.6, C^4H], 122.6−131.1 (m, CH of Ph), 134.5 [d, ^1J(C-P_B) = 84.1, C of Ph], 135.2 [d, ^1J(C-P_B) = 86.8, C of Ph], 141.4 (m, $C^{3,5}$), 155.5 (m, Cq de C_6H_5) ppm. ^{31}P NMR (121.5 MHz, $CDCl_3$, 298 K): δ = −0.31 [AB_2, t, ^2J(P_A-P_B) = 50.6, P_A], 37.36 [AB_2, d, ^2J(P_A-P_B) = 50.6, P_B] ppm. MS (EI): *m*/*z* = 682 [M^+ − ($NHEt_2$)]. $C_{45}H_{42}NP_3S_2$ (753.88): calcd. C 71.69, H 5.62; found C 41.26, H 5.17.

Complex 10: A mixture of [Pd(COD)Cl_2] (28 mg, 0.1 mmol) and **7** (71 mg, 0.1 mmol) in THF (10 mL) was stirred for 1 h at room temperature. After removing the solvent under vacuum, the resultant solid was washed first with hexanes (3 × 2 mL) then with diethyl ether (3 × 2 mL). After drying, **10** (78 mg) was recovered as a yellow solid in 92% yield. For characterization see ref.[21]

Complex 11: A mixture of [Pd(COD)Cl_2] (28 mg, 0.1 mmol) and **8** (71 mg, 0.1 mmol) in THF (10 mL) was stirred for 1 h at room temperature. After removing the solvent under vacuum, the so-obtained solid was washed first with hexanes (3 × 2 mL) and then with diethyl ether (3 × 2 mL). After drying, **11** (76 mg) was recovered as a yellow powder in 78% yield. ^{1}H NMR (300 MHz, CD_2Cl_2, 298 K): δ = 1.20 [t, ^3J(H−H) = 7.0, 3 H, CH_3], 4.30 [dq, ^2J(H-P_A) = 9, ^4J(H−H) = 7, 2 H, CH_2], 5.47 [t, ^3J(H-P_B) = 7.0, 1 H, H^4], 6.68−7.89 (m, 30 H, CH of Ph) ppm. ^{13}C NMR (75.5 MHz, CD_2Cl_2, 298 K): δ = 17.6 (m, CH_3), 66.0 [d, ^2J(C-P_A) = 4.6, CH_2], 95.9 [ddd, ^1J(C-P_A) = 91, ^1J(C-P_B) = 66.3, ^3J(C-$P_{B'}$) = 7.7, $C^{2,6}$], 116.1 [q, ^4J(C-P_A) = ^4J(C-P_B) = 12.2, C^4H], 128.8−129.9 (m, CH of Ph), 131.7 [dd, ^1J(C-P_B) = 84.3, ^3J(C-P_A) = 8.5, C of Ph], 132.8 [dd, ^1J(C-P_B) = 37.2, ^3J(C-P_A) = 3.8, C of Ph], 133.2−133.8 (m, CH of Ph), 141.5 [dt, ^2J(C-P_A) = 9.2, ^2J(C-P_B) = ^4J(C-$P_{B'}$) = 3.5, $C^{3,5}$], 155.5 [d, ^3J(C-P_A) = 2.3, C of Ph] ppm. ^{31}P NMR (121.5 MHz, CD_2Cl_2, 298 K): δ = 52.20 [AB_2, d, ^2J(P_A-P_B) = 103.0, P_B], 96.24 [AB_2, t, ^2J(P_A-P_B) = 103.0, P_A] ppm. $C_{43}H_{36}ClOP_3PdS_2$ (867.67): calcd. C 59.52, H 4.18; found C 59.14, H 3.79.

Pd Complex 12: A mixture of [Pd(COD)Cl_2] (37.9 mg, 0.13 mmol) and λ^5-phosphinine **9** (100 mg, 0.13 mmol) in CH_2Cl_2 (5 mL) was stirred for 30 min at room temperature. The so-obtained yellow precipitate was washed first with hexanes (3 × 2 mL) and then with diethyl ether (3 × 2 mL). After drying, complex **12** (114 mg) was recovered as a yellow solid in 90% yield . ^{1}H NMR (300 MHz, [D_6]acetone, 298 K): δ = 1.27 [t, $^3J_{H,H}$ = 6.3, 6 H, CH_3], 2.95 [dq, ^3J(H-P_A) = ^3J(H−H) = 6.3, 4 H, CH_2], 5.84 [dt, ^3J(H-P_A) = ^3J(H-P_B) = 3.5, 1 H, H^4], 6.66−7.70 (m, 30 H, CH of Ph), 9.25 (br. s, 1 H, NH) ppm. ^{31}P NMR (121.5 MHz, CH_2Cl_2, 298 K): δ = 49.32 [AB_2, d, ^2J(P_A-P_B) = 100.1, P_BPh_2], 82.18 [AB_2, t, ^2J(P_A-P_B) = 100.1, P_A]. **12** was too insoluble to give a satisfactory ^{13}C NMR spectrum. $C_{45}H_{42}Cl_2NP_3PdS_2$ (931.20): calcd. C 58.04, H 4.55; found C 57.91, H 4.37.

Pd Complex 13: A mixture of **1** (300 mg, 0.44 mmol) and [Pd(COD)Cl_2] (125 mg, 0.44 mmol) in CH_2Cl_2 (10 mL) was stirred for 15 min at room temperature. Menthol (6.9 mg, 0.44 mmol) was then added to the solution, which was stirred for a further hour at room temperature and then filtered through celite. After evaporation of the solvent, the resultant solid was washed first with hexanes (3 × 2 mL) and then with diethyl ether (3 × 2 mL). After drying, complex **13** was recovered as a yellow solid. Suitable crystals for X-ray structure analysis were grown by diffusion of hexanes into a solution of **13** in CH_2Cl_2. Yield 94%, 404 mg. ^{1}H NMR (300 MHz, CD_2Cl_2, 298 K): δ = 0.75 [d, ^3J(H−H) = 7.1, 3 H, CH_3], 0.87 [d, ^3J(H−H) = 6.2, 3 H, CH_3], 0.95 [d, ^3J(H−H) = 6.8, 3 H, CH_3], 1.08−1.75 (m, 8 H, CH and CH_2), 2.57 [d, ^2J(H−H) = 13.4, 1 H, CH_2], 4.78−4.87 (m, 1 H, OMen), 5.65 [t, ^4J(H-P_B) = 4.3, 1 H, H^4], 6.64−7.60 (m, 30 H, CH of Ph) ppm. ^{13}C NMR (75.5 MHz, CD_2Cl_2, 298 K): δ = 16.7 (s, CH_3), 20.4 (s, CH_3), 21.2 (s, CH_3), 22.4 (s, CH_2), 24.4 (s, CH), 31.3 (s, CH), 33.6 (s, CH_2), 44.2 (s, CH_2), 48.9 [d, ^3J(C-P_A) = 6.6, O−CH−CH], 77.2 [d, ^1J(C-P_A) = 6.4, O-CH], 116.6 [AB_2X, q, ^4J(C-P_A) = ^4J(C-P_B) = 10.7, C^4H], 127.0−128.2 (m, CH of Ph), 130.1 [dd, ^1J(C-P_B) = 83.3, ^3J(C-P_A) = 7.6, C of Ph], 130.4 [dd, ^1J(C-P_B) = 84.3, ^3J(C-P_A) = 7.2, C of Ph], 131.2−132.1 (m, CH of Ph), 139.2 (m, $C^{3,5}$), 155.8 (br. s, C of Ph), 156.4 (br. s, C of Ph). C^2 and C^6 not observed. ^{31}P NMR (121.5 MHz, CD_2Cl_2, 298 K): δ = 47.67 [ABB′, d, ^2J(P_A-P_B) = 111.3, P_B], 49.89 [ABB′, d, ^2J(P_A-$P_{B'}$) = 104.1, $P_{B'}$], 88.24 [ABB′, dd, ^2J(P_A-P_B) = 111.3, ^2J(P_A-$P_{B'}$) = 104.1, P_A] ppm. $C_{51}H_{50}ClONP_3PdS_2$ (977.87): calcd. C 62.64, H 5.15; found C 62.19, H 4.84.

Pd Complex 14: A mixture of **1** (100 mg, 0.15 mmol) and [Pd(COD)Cl_2] (42 mg, 0.15 mmol) in THF (5 mL) was stirred for 15 min at room temperature. In a glove-box, Et_2NLi (15 mg, 0.19 mmol) was added to the solution which was then stirred for 30 min at room temperature. The solvent was subsequently removed under vacuum and the resultant solid washed first with hexanes (3 × 2 mL) and then with diethyl ether (3 × 2 mL). After evaporation of the solvent, the resulting solid was dissolved in CH_2Cl_2 and filtered through celite. After drying, complex **14** was recovered as a yellow solid. Suitable crystals for X-ray structure analysis were grown by diffusion of hexanes into a solution of CH_2Cl_2. Yield: 89%, 132 mg. ^{1}H NMR (300 MHz, CD_2Cl_2, 298 K): δ = 1.14 [t, ^3J(H−H) = 7.1, 6 H, CH_3], 4.30 [dq, ^3J(H-P_A) = 11.3, ^4J(H−H) = 7.1, 4 H, CH_2], 5.45 [t, ^4J(H-P_B) = 4.9, H^4], 6.71−7.52 (m, 30 H, CH of Ph) ppm. ^{13}C NMR (75.5 MHz, CD_2Cl_2, 298 K): δ = 11.1 (s, CH_3), 42.1 (m, CH_2), 89.1 [ddd, ^1J(C-P_A) = 89.0, ^1J(C-P_B) = 64.3, ^3J(C-$P_{B'}$) = 7.6, $C^{2,6}$], 115.0 [td, ^4J(C-P_B) = 10.3, ^4J(C-P_A) = 2.9, C^4H], 127.6−128.8 (m, CH of Ph), 131.6 [dd, ^1J(C-P_B) = 78.9, ^3J(C-P_A) = 5.4, C of Ph], 132.4 [dd, ^1J(C-P_B) = 84.3, ^3J(C-P_A) = 5.7, C of Ph], 132.1−132.7 (m, C of Ph), 141.5 [m,

Σ^2J(C-P) = 14.8, $C^{3,5}$], 155.5 (m, C of Ph) ppm. ^{31}P NMR (121.5 MHz, CH_2Cl_2, 298 K): δ = 51.77 [AB_2, d, $^2J(P_A\text{-}P_B)$ = 100.0, P_B], 66.46 [AB_2, t, $^2J(P_A\text{-}P_B)$ = 100.0, P_A] ppm. $C_{45}H_{41}ClNP_3PdS_2$ (894.74): calcd. C 60.41, H 4.62; found C 59.96, H 4.13.

Anion 15: A solution of MeLi in Et_2O (1.8 mL, C = 0.16 M, 0.29 mmol) was added by syringe into a solution of **1** (200 mg, 0.29 mmol) in THF (10 mL) at −78 °C. The solution was then warmed to room temperature and stirred for 20 min. After drying, **15** (206 mg) was recovered as a red solid in 100% yield. ^{1}H NMR (300 MHz, [D$_8$]THF, 298 K): δ = 0.99 [d, $^2J(H\text{-}P_A)$ = 3.4, 3 H, CH_3], 5.13 [t, $^4J(H\text{-}P_B)$ = 4.8, 1 H, H^4], 6.53−7.57 (m, 30 H, CH of Ph) ppm. ^{31}P NMR (121.5 MHz, [D$_8$]THF, 298 K): δ = 45.87 [AB_2, d, $^2J(P_A\text{-}P_B)$ = 155.5, P_B], −65.70 [AB_2, t, $^2J(P_A\text{-}P_B)$ = 155.5, P_AMe].

λ^5-Phosphinine 16: A solution of MeLi in Et_2O (1.8 mL, C = 0.16 M, 0.29 mmol) was added by syringe into a solution of **1** (200 mg, 0.29 mmol) in THF (10 mL) at −78 °C. The solution was then warmed to room temperature and stirred for 20 min. Complete formation of **15** was checked by ^{31}P NMR spectroscopy. After cooling at −78 °C, C_2Cl_6 (69 mg, 0.29 mmol) was added and the resultant solution was warmed to room temperature and stirred for a further 20 min. After removing the solvent, the solid was washed first with hexanes (3 × 2 mL) and then with diethyl ether (3 × 2 mL). The so-obtained solid was then dissolved in CH_2Cl_2 and filtered through celite. After drying, **16** (201 mg) was recovered as a yellow solid in 95% yield. ^{1}H NMR (300 MHz, [D$_8$]THF, 298 K): δ = 2.04 [d, $^2J(H\text{-}P_A)$ = 15.1, 3 H, CH_3], 6.16 [vq, $^4J(H\text{-}P_B)$ = $^4J(H\text{-}P_B)$ = 4.1, 1 H, H^4], 6.97−8.15 (m, 30 H, CH of Ph) ppm. ^{13}C NMR (75.5 MHz, [D$_8$]THF, 298 K): δ = 18.6 [d, $^1J(C\text{-}P_A)$ = 67.3, CH_3], 83.8 [dd, $^1J(C\text{-}P_A)$ = 90.9, $^1J(C\text{-}P_B)$ = 83.1, $^3J(C\text{-}P_{B'})$ = 3.2, $C^{2,6}$], 117.7 [dt, $^3J(C\text{-}P_A)$ = 27.8, $^3J(C\text{-}P_B)$ = 9.0, C^4H], 128.5−138.7 (m, C and CH of Ph), 143.5 [m, ΣJ(C-P) = 18.3, $C^{3,5}$], 157.6 [d, ^3J(C-P) = 5.3, C of Ph] ppm. ^{31}P NMR (121.5 MHz, [D$_8$]THF, 298 K): δ = 65.62 [AB_2, t, $^2J(P_A\text{-}P_B)$ = 42.5, P_A], 35.16 [AB_2, d, $^2J(P_A\text{-}P_B)$ = 42.5, P_B] ppm. MS (EI): m/z = 732 [M$^+$]. **16** was too moisture sensitive to give satisfactory elemental data.

Pd Complex 17: A mixture of [Pd(dba)$_2$] (79 mg, 0.14 mmol) and **16** (100 mg, 0.14 mmol) in CH_2Cl_2 (5 mL) was stirred for 30 min at room temperature. After evaporation of the solvent, the resultant solid was washed first with hexanes (3 × 2 mL) and then with diethyl ether (3 × 2 mL). After drying, **17** (108 mg) was recovered as a brown powder in 92% yield. ^{1}H NMR (300 MHz, CD_2Cl_2, 298 K): δ = 1.88 [d, $^2J(H\text{-}P_A)$ = 9.6, 3 H, CH_3], 5.42 [t, $^4J(H\text{-}P_B)$ = 4.4, 1 H, H^4], 6.61−7.47 (m, 30 H, CH of Ph) ppm. ^{13}C NMR (75.5 MHz, CD_2Cl_2, 298 K): δ = 24.3 (m, CH_3), 74.2 [dd, $^1J(C\text{-}P_A)$ = 97.4, $^1J(C\text{-}P_B)$ = 53.0, $C^{2,6}$], 117.7 [m, ΣJ(C-P) = 36.5, C^4H], 127.6−132.5 (m, C and CH of Ph), 141.5 [m, ΣJ(C-P) = 23.1, $C^{3,5}$], 158.9 (s, C of Ph) ppm. ^{31}P NMR (121.5 MHz, CD_2Cl_2, 298 K): δ = 49.44 [AB_2, m, $^2J(P_A\text{-}P_B)$ = 35.0, P_A], 50.44 [AB_2, m, $^2J(P_A\text{-}P_B)$ = 35.0, P_B] ppm. $C_{42}H_{34}ClP_3PdS_2$ (837.65): calcd. C 60.22, H 4.09; found C 59.83, H 3.86.

Ni Complex 18: A mixture of [Ni(dme)Br$_2$] (136 mg, 0.44 mmol) and **1** (300 mg, 0.44 mmol) in CH_2Cl_2 (10 mL) was stirred for 1 h at 40 °C. After evaporation of the solvent, the resulting solid was washed with hexanes (3 × 2 mL) and, after drying, complex **18** (384 mg) was then recovered as a brown powder in 97% yield. ^{31}P NMR (121.5 MHz, CD_2Cl_2, 298 K): δ = 55.92 [AB_2, d, $^2J(P_A\text{-}P_B)$ = 137.4, P_BPh_2], 98.52 [AB_2, t, $^2J(P_A\text{-}P_B)$ = 137.4, P_A]. Complex **18** was too moisture sensitive to give satisfactory elemental data.

Pt Complex 19: A mixture of [Pt(COD)Cl$_2$] (165 mg, 0.44 mmol) and **1** (300 mg, 0.44 mmol) in CH_2Cl_2 (10 mL) was stirred for 15 min at room temperature. After evaporation of the solvent, the resulting solid was washed with hexanes (3 × 2 mL) and then dried to afford complex **19** (400 mg) as a yellow powder in 96% yield. ^{31}P NMR (121.5 MHz, CD_2Cl_2, 298 K): δ = 47.99 [AB_2, d, $^2J(P_A\text{-}P_B)$ = 109.1, P_B], 67.10 [AB_2M, td, $^1J(P_A\text{-Pt})$ = 3860.3, $^2J(P_A\text{-}P_B)$ = 109.1, P_A].

Ni Complex 20: A solution of [Ni(dme)Br$_2$] (136 mg, 0.44 mmol) and **1** (300 mg, 0.44 mmol) in CH_2Cl_2 (10 mL) was stirred for 30 min at room temperature and then ethanol (200 μL, 3.4 mmol) was added. After stirring for 15 min at room temperature, the solvent was removed under vacuum and the resulting solid was washed first with hexanes (3 × 2 mL) and then with diethyl ether (3 × 2 mL). After drying, complex **20** (365 mg) was recovered as a brown powder in 96% yield. ^{1}H NMR (300 MHz, CD_2Cl_2, 298 K): δ = 1.27 [d, $^3J(H\text{−}H)$ = 7.0, CH_3], 4.52 [AB_2X, dq, $^3J(H\text{−}H)$ = $^3J(H\text{-}P_A)$ = 7.2, 2 H, CH_2], 6.73−7.82 (m, 31 H, H^4 and CH of Ph) ppm. ^{13}C NMR (75.5 MHz, CD_2Cl_2, 298 K): δ = 16.4 [d, $^3J(C\text{-}P_A)$ = 8.0, CH_3], 65.4 [d, $^2J(C\text{-}P_A)$ = 4.0, CH_2], 95.9 [m, ΣJ(C-P) = 158.1, $C^{2,6}$], 114.8 [q, $^3J(C\text{-}P_A)$ = $^3J(C\text{-}P_B)$ = 10.1, C^4H], 127.6−132.5 (m, C and CH of Ph), 140.9 [p, $^2J(C\text{-}P_A)$ = $^2J(C\text{-}P_B)$ = $^4J(C\text{-}P_{B'})$ = 3.4, $C^{3,5}$], 154.4 (s, C of Ph) ppm. ^{31}P NMR (121.5 MHz, CD_2Cl_2, 298 K): δ = 58.26 [AB_2, d, $^2J(P_A\text{-}P_B)$ = 123.9, P_B], 104.57 [AB_2, t, $^2J(P_A\text{-}P_B)$ = 123.9, P_A] ppm. $C_{43}H_{36}BrNiOP_3S_2$ (864.40): calcd. C 59.75, H 4.20; found C 59.29, H 3.80.

Pt Complex 21: A solution of [Pt(COD)Cl$_2$] (165 mg, 0.44 mmol) and **1** (300 mg, 0.44 mmol) in CH_2Cl_2 (10 mL) was stirred for 15 min at room temperature and ethanol (200 μL, 3.4 mmol) was then added. After stirring for a further 15 min at room temperature, the solvent was removed under vacuum and the resulting solid was washed first with hexanes (3 × 2 mL) and then with diethyl ether (3 × 2 mL). After drying, complex **21** (400 mg) was recovered as a yellow powder in 95% yield. ^{1}H NMR (300 MHz, CD_2Cl_2, 298 K): δ = 1.38 [d, $^3J(H\text{−}H)$ = 7.0, CH_3], 4.31 [dq, $^3J(H\text{-}P_A)$ = 9.0, $^3J(H\text{−}H)$ = 7.0, 2 H, CH_2], 5.66 [dt, $^4J(H\text{-}P_B)$ = 4.8, $^4J(H\text{-}P_A)$ = 0.8, 1 H, H^4], 6.69−7.67 (m, 30 H, CH of Ph) ppm. ^{13}C NMR (75.5 MHz, CD_2Cl_2, 298 K): δ = 16.6 [d, $^3J(C\text{-}P_A)$ = 7.3, CH_3], 62.7 [d, $^2J(C\text{-}P_A)$ = 5.0, CH_2], 88.8 [ddd, $^1J(C\text{-}P_A)$ = 92.6, $^1J(C\text{-}P_B)$ = 80.0, $^3J(C\text{-}P_{B'})$ = 5.0, $C^{2,6}$], 116.3 [q, $^4J(C\text{-}P_A)$ = $^4J(C\text{-}P_B)$ = 12.8, C^4H], 127.6−128.8 (m, CH of Ph), 130.7 [dd, $^1J(C\text{-}P_B)$ = 83.9, $^3J(C\text{-}P_A)$ = 5.7, C of Ph], 131.5 [dd, $^1J(C\text{-}P_B)$ = 86.6, $^3J(C\text{-}P_A)$ = 3.4, C of Ph], 132−132.8 (m, C of Ph), 140.5 [dt, $^2J(C\text{-}P_A)$ = 8.3, $^2J(C\text{-}P_B)$ = $^4J(C\text{-}P_{B'})$ = 2.9, $C^{3,5}$], 155.5 (s, C of Ph) ppm. ^{31}P NMR (121.5 MHz, CD_2Cl_2, 298 K): δ = 48.86 [AB_2M, d, $^2J(P_A\text{-}P_B)$ = 98.5, P_B], 65.47 [AB_2M, t, $^1J(P_A\text{-Pt})$ = 3640.0, $^2J(P_A\text{-}P_B)$ = 98.5, P_A] ppm. $C_{43}H_{36}ClOP_3PtS_2$ (956.33): calcd. C 54.00, H 3.79; found C 53.64, H 3.48.

Ni Complex 22: A solution of *n*BuLi in hexanes (0.275 mL, C = 1.6 M, 0.44 mmol) was added by syringe into a solution of **1** (300 mg, 0.44 mmol) in THF (10 mL) at −78 °C. The resultant solution was then warmed to room temperature and stirred for 20 min. Complete formation of **3** was checked by ^{31}P NMR (121.5 MHz, THF, 298 K): δ = 45.80 [AB_2, d, ^2J(P-P) = 156.0, P_BPh_2], −66.20 [AB_2, t, $^2J(P_A\text{-}P_B)$ = 156.0, P_A-*n*Bu]. After cooling at −78 °C, [Ni(dme)Br$_2$] (136 mg, 0.44 mmol) was added and the solution was warmed to room temperature and stirred for 15 min. The solvent was then removed and the resulting solid was dissolved in CH_2Cl_2 (8 mL) and filtered through celite. After evaporating the solvent under vacuum, the solid was washed several times with hexanes (3 × 2 mL) and diethyl ether (3 × 2 mL). After drying, **22** was recovered as a

brown solid. Suitable crystals for X-ray structure analysis were grown from a diffusion of hexanes into a solution of CH_2Cl_2. Yield: 91%, 350 mg. ^{1}H NMR (300 MHz, CD_2Cl_2, 298 K): δ = 0.97 [t, ^3J(H-H) = 7.2, 3 H, CH_3], 1.53 (m, 2 H, CH_2), 2.00 (br. s, 4 H, CH_2), 5.38 [t, ^4J(H-P_B) = 4.2, 1 H, H^4], 6.62−7.44 (m, 30 H, CH of Ph) ppm. ^{13}C NMR (75.5 MHz, CD_2Cl_2, 298 K): δ = 12.8 (s, CH_3), 23.2 [d, ^3J(C-P_A) = 13.7, CH_2], 25.2 (s, CH_2), 38.9 [d, ^1J(C-P_A) = 25.7, CH_2], 72.5 (m, $C^{2,6}$), 118.6 (m, C^4H), 126.7−132.0 (m, CH and C of C_6H_5), 139.4 [d, ^2J(C-P_A) = 6.8, $C^{3,5}$], 158.1 (s, C of C_6H_5) ppm. ^{31}P NMR (121.5 MHz, THF, 298 K): δ = 57.34−63.09 (m, AB_2) ppm. $C_{45}H_{40}BrNiP_3S_2$ (876.45): calcd. C 61.67, H 4.60; found C 61.31, H 4.24.

Pt Complex 23: A solution of *n*BuLi in hexanes (0.275 mL, C = 1.6 M, 0.44 mmol) was added by syringe into a solution of **1** (300 mg, 0.44 mmol) in THF (10 mL) at −78 °C. The resultant solution was then warmed to room temperature and stirred for 20 min. Complete formation of **3** was checked by ^{31}P NMR spectroscopy. After cooling at −78 °C, [Pt(COD)Cl_2] (165 mg, 0.44 mmol) was added and the solution was warmed to room temperature and stirred for 15 min. The solvent was then evaporated and the resulting solid was dissolved in CH_2Cl_2 (8 mL) and filtered through celite. After removing the solvent under vacuum, the solid was washed several times with hexanes (3 × 2 mL) and diethyl ether (3 × 2 mL), and, after drying, **23** (392 mg) was recovered as a yellow solid in 92% yield. ^{1}H NMR (300 MHz, CD_2Cl_2, 298 K): δ = 1.1−2.22 (m, 9 H, CH_3 and CH_2), 5.60 [br. d, ^4J(H-P_A) = 2.4, 1 H, H^4], 6.70−7.70 (m, 30 H, CH of C_6H_5) ppm. ^{31}P NMR (121.5 MHz, THF, 298 K): δ = 21.52 [AB_2M, td, ^2J(P_A-Pt) = 3030.6, ^2J(P_A-P_B) = 81.0, P_A], 46.95 [AB_2M, d, ^2J(P_A-P_B) = 87.0, P_B]. **24** was too insoluble in common solvents to give a satisfactory ^{13}C NMR spectrum. $C_{45}H_{40}ClP_3PtS_2$ (968.38): calcd. C 55.81, H 4.16; found C 55.43, H 3.75.

Pd Complex 24: Acetonitrile (50 μL, 0.96 mmol) was added to a mixture of **4** (150 mg, 0.17 mmol) and $AgBF_4$ (37 mg, 0.19 mmol) in CH_2Cl_2 (5 mL). The resultant solution was stirred for 15 min at room temperature and was then filtered through celite. After drying, **24** (140 mg) was recovered as an orange powder in 85% yield. ^{1}H NMR (300 MHz, CD_2Cl_2, 298 K): δ = 1.05 [t, ^3J(H−H) = 7.3, 3 H, CH_3 of *n*Bu], 1.62 [qt, ^3J(H−H) = 14.6, ^3J(H−H) = 7.3, CH_2], 2.03 (m, 2 H, CH_2), 2.26 (m, 2 H, CH_2), 2.23 (s, 3 H, CH_3 of CH_3CN), 2.44 (m, 2 H, CH_2), 5.60 [t, ^4J(H-P_B) = 5.1, 1 H, H^4], 6.69−7.89 (m, 30 H, CH of Ph) ppm. ^{13}C NMR (75.5 MHz, CD_2Cl_2, 298 K): δ = 8.6 (s, CH_3 of CH_3CN), 13.4 (s, CH_3 of *n*Bu), 23.5 [d, ^3J(C-P_A) = 17.2, CH_2], 25.7 [d, ^2J(C-P_A) = 15.7, CH_2], 45.2 [d, ^1J(C-P_A) = 38.2, CH_2], 71.5 (m, $C^{2,6}$), 119.3 (m, C^4H), 126.2 [d, ^2J(C-P_A) = 25.5, C of CH_3CN], 125.2−134.5 (m, CH and C of Ph), 138.4 [ABB′X, dt, ^2J(C-P_A) = ^2J(C-P_B) = 9.0, ^4J(C-$P_{B'}$) = 3.1, $C^{3,6}$], 163 (m, C of Ph) ppm. ^{31}P NMR (121.5 MHz, THF, 298 K): δ = 49.72 [AB_2, d, ^2J(P_A-P_B) = 69.6, P_BPh_2], 64.61 [AB_2, t, ^2J(P_A-P_B) = 69.6, P_A] ppm. $C_{47}H_{43}BF_4NP_3PdS_2$ (972.13): calcd. C 58.07, H 4.46; found C 57.67, H 4.02.

Pd Complex 25: Acetonitrile (50 μL, 0.96 mmol) was added to a mixture of **11** (148 mg, 0.17 mmol) and $AgBF_4$ (37 mg, 0.19 mmol) in CH_2Cl_2 (5 mL). After stirring for 15 min at room temperature, the solution was filtered through celite. After drying, **25** (155 mg) was recovered as an orange powder in 95% yield. ^{1}H NMR (300 MHz, CD_2Cl_2, 298 K): δ = 1.35 [t, ^3J(H−H) = 7.0, 3 H, CH_3 of EtO], 2.20 (s, 3 H, CH_3 of CH_3CN), 4.22 [dq, ^3J(H-P_A) = 1.2, ^3J(H−H) = 7.0, 2 H, CH_2], 5.71 [t, ^4J(H-P_B) = 4.9, 1 H, H^4], 6.69−7.79 (m, 30 H, CH of Ph) ppm. ^{13}C NMR (75.5 MHz, CD_2Cl_2, 298 K): δ = 2.3 (s, CH_3), 16.2 [d, ^3J(C-P_A) = 8.6, CH_3], 66.9 [d, ^2J(C-P_A) = 8.1, CH_2], 91.6 [ddd, ^1J(C-P_A) = 93.2, ^1J(C-P_B) = 71.0, ^3J(C-$P_{B'}$) = 7.7, $C^{2,6}$], 117.1 [q, ^4J(C-P_A) = ^4J(C-P_B) = 12.2, C^4H], 121.2 (br. s, C of CH_3CN), 127.8 [dd, ^1J(C-P_B) = 84.7, ^3J(C-P_A) = 7.4, C of Ph], 128.1 [ABX, d, ^1J(C-P_B) = 86.6, C of Ph], 128.1−134.8 (m, CH of Ph), 139.0 [dt, ^2J(C-P_A) = 9.1, ^2J(C-P_B) = ^4J(C-$P_{B'}$) = 3.5, $C^{3,5}$], 160.5 (s, C of Ph) ppm. ^{31}P NMR (121.5 MHz, THF, 298 K): δ = 49.03 [AB_2, d, ^2J(P_A-P_B) = 85.5, P_B], 87.81 [AB_2, t, ^2J(P_A-P_B) = 85.5, P_A] ppm. $C_{45}H_{39}BF_4NOP_3PdS_2$ (960.08): calcd. C 56.30, H 4.09; found C 55.84, H 3.75.

Ni Complex 26: Acetonitrile (50 μL, 0.96 mmol) was added to a mixture of **20** (138 mg, 0.16 mmol) and $AgBF_4$ (37 mg, 0.19 mmol) in CH_2Cl_2 (5 mL), and the resultant solution was stirred for 15 min at room temperature. The solution was then filtered through celite and, after drying, **26** was recovered as a brown powder (yield: 92%, 134 mg). ^{1}H NMR (300 MHz, CD_2Cl_2, 298 K): δ = 1.20 (br. s, 3 H, CH_3 of Et), 2.30 (br. s, 3 H, CH_3 of CH_3CN), 4.15 (br. s, 2 H, CH_2), 5.60 (br. s, 1 H, H^4), 6.40−7.80 (m, 30 H, CH of Ph) ppm. ^{13}C NMR (75.5 MHz, CD_2Cl_2, 298 K): δ = 7.8 (s, CH_3 of CH_3CN), 15.7 [s, ^3J(C-P_A) = 8, CH_3 of Et], 64.6 [d, ^2J(C-P_A) = 6.9, CH_2], 91.9 (m, $C^{2,6}$), 115.1 [q, ^4J(C-P_A) = ^4J(C-P_B) = 9.8, C^4H], 127.19−132.4 (m, CH and C of Ph and C of CH_3CN), 139.0 [dt, ^4J(C-P_B) = 8, ^2J(C-P_A) = ^2J(C-P_B) = 4, $C^{3,5}$], 156.5 (s, C of Ph) ppm. ^{31}P NMR (121.5 MHz, THF, 298 K): δ = 55.22 [AB_2, d, ^2J(P_A-P_B) = 106.3, P_B], 88.79 [AB_2, t, ^2J(P_A-P_B) = 106.3, P_A] ppm. $C_{45}H_{39}BF_4NNiOP_3S_2$ (912.35): calcd. C 59.24, H 4.31; found C 58.79, H 3.92.

Pt Complex 27: Acetonitrile (50 μL, 0.96 mmol) was added to a mixture of **21** (153 mg, 0.16 mmol) and $AgBF_4$ (37 mg, 0.19 mmol) in CH_2Cl_2 (5 mL). After stirring for 15 min at room temperature, the solution was filtered through celite. After drying, **27** was recovered as a yellow powder (yield: 93%, 156 mg). ^{1}H NMR (300 MHz, CD_2Cl_2, 298 K): δ = 1.49 [t, ^3J(H−H) = 7.0, 3 H, CH_3 of Et], 2.37 (s, 3 H, CH_3 of CH_3CN), 4.15 [p, ^3J(H-P_B) = ^3J(H−H) = 7.0, 2 H, CH_2], 5.97 [t, ^4J(H-P_B) = 5.1, 1 H, H^4], 6.75−7.82 (m, 30 H, CH of Ph) ppm. ^{13}C NMR (75.5 MHz, CD_2Cl_2, 298 K): δ = 3.5 (s, CH_3), 16.5 [d, ^3J(C-P_A) = 7.5, CH_3], 65 [d, ^2J(C-P_A) = 9.8, CH_2], 84.5 [ddd, ^1J(C-P_A) = 96.8, ^1J(C-P_B) = 87.2, ^3J(C-$P_{B'}$) = 5.6, $C^{2,6}$], 118.5 [q, ^4J(C-P_A) = ^4J(C-P_B) = 2.1, C^4H], 125.0 [d, ^2J(C-P_A) = 21.4, C of CH_3CN], 127 [dd, ^1J(C-P_B) = 91.0, ^3J(C-P_A) = 4.1, C of Ph], 128 [dd, ^1J(C-P_B) = 95.7, ^3J(C-P_A) = 3.7, C of Ph], 128.1−134.8 (m, CH of Ph), 139 (m, $C^{3,5}$), 160.5 (s, C of Ph) ppm. ^{31}P NMR (121.5 MHz, THF, 298 K): δ = 48.92 [AB_2M, d, ^2J(P_A-P_B) = 80.4, P_B], 54.60 [AB_2M, ptt, ^1J(P_A-Pt) = 3592.9, ^2J(P_A-P_B) = 75.2, P_A] ppm. $C_{45}H_{39}BF_4NOP_3PtS_2$ (1048.73): calcd. C 51.54, H 3.75; found C 51.29, H 3.24.

Pd Complex 28: A mixture of **4** (97 mg, 0.11 mmol) and AgOTf (37 mg, 0.19 mmol) was stirred in CH_2Cl_2 (3 mL) for 15 min at room temperature and filtered through celite. After drying, **28** was recovered as a red powder (yield: 87%, 95 mg). ^{1}H NMR (300 MHz, CD_2Cl_2, 298 K): δ = 1.05 [t, ^3J(H−H) = 6.9, 3 H, CH_3], 1.62 [qt, ^3J(H−H) = 6.9, ^3J(H−H) = 13.8, CH_2], 1.92−2.06 (m, 2 H, CH_2), 2.19−2.31 (m, 2 H, CH_2), 5.50 [t, ^4J(H-P_B) = 4.7, 1 H, H^4], 6.68−7.56 (m, 30 H, CH of Ph) ppm. ^{13}C NMR (75.5 MHz, CD_2Cl_2, 298 K): δ = 13.9 (s, CH_3 of *n*Bu), 23.5 [d, ^3J(C-P_A) = 2.6, CH_2], 25.5 [d, ^2J(C-P_A) = 2.6, CH_2], 38.3 (m, CH_2), 71.6 (m, $C^{2,6}$), 118.6 [q, ^4J(C-P_A) = ^4J(C-P_B) = 10.6, C^4H], 127.7−128.8 (m, CH of Ph), 131.1 [dd, ^1J(C-P_B) = 83.8, ^3J(C-P_A) = 8.3, C of Ph], 131.9−133.0 (m, CH of Ph), 139.6 (m, $C^{3,5}$), 159.5 ppm (m, C of Ph), CF_3 not observed. ^{31}P NMR (121.5 MHz, THF, 298 K): δ = 49.47 [AB_2, d, ^2J(P_A-P_B) = 84.4, P_B], 56.05 [AB_2,

t, $^2J(P_A\text{-}P_B)$ = 84.4, P_A] ppm. $C_{46}H_{40}F_3O_3P_3PdS_3$ (993.34): calcd. C 55.62, H 4.06; found C 55.43, H 3.86.

λ⁵-Dimethylphosphinine 29: A solution of MeLi in hexanes (275 μL, *C* = 1.6 M, 0.44 mmol) was added by syringe into a solution of **1** (300 mg, 0.44 mmol) in THF (10 mL) at −78 °C. The resultant solution was then warmed to room temperature and stirred for 20 min. Complete formation of **15** was checked by ^{31}P NMR (121.5 MHz, THF, 298 K): δ = 44.83 [AB_2, d, $^2J(P_A\text{-}P_B)$ = 156.7, P_B], −66.52 [AB_2, t, $^2J(P_A\text{-}P_B)$ = 156.7, P_A]. After cooling at −78 °C, MeI (50 μL, 0.80 mmol) was added and the solution was warmed to room temperature and stirred for 15 min. The solvent was then evaporated and the resulting solid was dissolved in CH_2Cl_2 (8 mL) and filtered through celite. After removing the solvent under vacuum, the solid was washed several times with hexanes (3 × 2 mL) and then diethyl ether (3 × 2 mL). After drying, **29** was recovered as an orange powder. Suitable crystals for X-ray structure analysis were grown by diffusion of hexanes into a solution of $CDCl_3$.Yield: 89%, 278 mg. ^1H NMR (300 MHz, $CDCl_3$, 298 K): δ = 1.64 [d, $^2J(P_A-H)$ = 13.4, 6 H, CH_3], 5.34 [t, $^4J(H\text{-}P_B)$ = 4.8, 1 H, H^4], 6.71−7.81 (m, 30 H, CH of Ph) ppm. ^{13}C NMR (75.5 MHz, $CDCl_3$, 298 K): δ = 12.2 [d, $^1J(C\text{-}P_A)$ = 58.4, CH_3], 67.0 [ddd, $^1J(C\text{-}P_A)$ = 88.8, $^1J(C\text{-}P_B)$ = 76.9, $^3J(C\text{-}P_{B'})$ = 2.9, $C^{2,6}$], 118.5 [m, ΣJ(C-P) = 42.8, C^4H], 127.6−131.9 (m, CH of Ph), 136.5 [dd, $^1J(C\text{-}P_B)$ = 85.4, $^3J(C\text{-}P_A)$ = 2.5, C of Ph], 142.8 [ddd, $^2J(C\text{-}P_A)$ = 10.9, $^2J(C\text{-}P_B)$ = 6.9, $^4J(C\text{-}P_{B'})$ = 3.3,$C^{3,5}$], 157.8 (s, C of Ph) ppm. ^{31}P NMR (121.5 MHz, THF, 298 K): δ = 20.77 [AB_2, t, $^2J(P_A\text{-}P_B)$ = 41.1, P_A], 37.44 [AB_2, d, $^2J(P_A\text{-}P_B)$ = 41.1, P_B] ppm. MS (EI): *m*/*z* = 712 [M^+]. $C_{43}H_{37}P_3S_3$ (710.81): calcd. C 72.66 H, 5.25; found C 72.28 H, 4.91.

Anion 30: In a glove-box, a mixture of **1** (150 mg, 0.22 mmol) and MeONa (36 mg, 0.66 mmol) in THF (5 mL) was stirred for 15 min. After drying, **30** was recovered as a yellow powder. Suitable crystals for X-ray structure analysis were grown from a diffusion of hexanes into a solution of THF. ^{31}P NMR (121.5 MHz, THF, 298 K): δ = 44.60 [AB_2, d, $^2J(P_A\text{-}P_B)$ = 153.2, P_B], 66.55 [AB_2, dd, $^2J(P_A\text{-}P_B)$ = 148.4, P_A] ppm. **30** was too moisture sensitive to give satisfactory elemental data.

X-ray Crystallographic Study: Crystals of compounds **1** (Table 5), **5**, **6**, **13** (Table 6), **14**, **22** (Table 7), **29** and **30** (Table 5) suitable for X-ray diffraction were obtained by slow diffusion of hexanes into a CH_2Cl_2 solution for **1**, **5**, **13**, **14**, **22**, into a $CDCl_3$ solution for **6**, **29**, and into a THF solution for **30**. Data were collected at 150.0(1) K on a Nonius Kappa CCD diffractometer using a Mo-*K*α (λ = 0.71070 Å) X-ray source and a graphite monochromator. All data were measured using phi and omega scans. Experimental details are described in tables 1, 3 and 4. The crystal structures were solved using SIR 97[45] and Shelxl-97.[46] ORTEP drawings were made using ORTEP III for Windows.[47] CCDC-210894 to 210900 and 210982 contain the supplementary crystallographic data for this paper. These data can be obtained free of charge at www.ccdc.cam.ac.uk/conts/retrieving.html [or from the Cambridge Crystallographic Data Centre, 12 Union Road, Cambridge CB2 1EZ, UK; fax: (internat.) +44−1223/336-033; E-mail: deposit@ccdc.cam.ac.uk].

Theoretical Methods: The calculations were performed with the GAUSSIAN 98 series of programs.[48] The geometries of compounds I and II were optimized using the gradient-corrected

Table 5. Crystal data and structural refinement details for **1**, **29**, **30**

	1	**29**	**30**
Empirical formula	$C_{41}H_{31}P_3S_2{\cdot}CH_2Cl_2$	$C_{43}H_{37}P_3S_2{\cdot}CHCl_3$	$C_{42}H_{34}OP_3S_2{\cdot}C_{18}H_{36}N_2O_6Na$
M_r	765.61	830.12	1111.20
T [K]	150.0(1)	150.0(1)	150.0(1)
Crystal system	monoclinic	monoclinic	triclinic
Space group	$P2_1/n$	$P2_1/n$	$P\bar{1}$
a [Å]	9.4560(10)	9.225(5)	9.127(1)
b [Å]	28.7580(10)	17.593(5)	17.624(1)
c [Å]	13.5950(10)	24.926(5)	17.900(1)
α [°]	90	90	94.980(1)
β [°]	95.5600(10)	92.167(5)	98.650(1)
γ [°]	90	90	96.410(1)
V [Å^3]	3679.6(5)	4042(3)	2813.0(4)
Z	4	4	2
ρ [g cm^{-3}]	1.382	1.364	1.312
μ [cm^{-1}]	0.452	0.481	0.242
Crystal size [mm]	0.22 × 0.09 × 0.09	0.18 × 0.18 × 0.12	0.20 × 0.16 × 0.10
F(000)	1584	1720	1176
Index ranges	$-11 \le h \le 11$; $35 \le k \le 34$; $-16 \le l \le 16$	$-12 \le h \le 12$; $21 \le k \le 23$; $-31 \le l \le 33$	$-9 \le h \le 10$; $-19 \le k \le 19$; $19 \le l \le 19$
Scan type	phi and omega	phi	phi and omega
$2\Theta_{max}$ [°]/criterion	26.37/>2σ*I*	28.70/>2σ*I*	22.98/>2σ*I*
Param. refined; data/param.	442; 12	471; 16	677; 8
Reflections collected	13188	17199	13666
Independent reflections	7483	10430	7760
Reflections used	5431	7671	5963
*wR*2	0.1168	0.1098	0.2142
*R*1	0.0437	0.0415	0.0784
Goodness of fit	1.040	1.048	1.054
Largest diff. peak / hole [e·Å^{-3}]	0.352(0.067) / −0.616(0.067)	0.335(0.064) / −0.571(0.064)	0.688(0.093) / −0.475(0.093)

Table 6. Crystal data and structural refinement details for **6**, **13**

	6	**13**
Empirical formula	$C_{41}H_{32}ClOP_3PdS_2 \cdot CH_2Cl_2$	$C_{51}H_{50}Cl_3OP_3PdS_2 \cdot CH_2Cl_2$
M_r	924.47	1062.72
T [K]	150.0(1)	150.0(1)
Crystal system	monoclinic	orthorhombic
Space group	$P2_1/n$	$P2_12_12_1$
a [Å]	15.644(5)	9.597(5)
b [Å]	12.229(5)	18.767(5)
c [Å]	21.024(5)	26.834(5)
β [°]	96.100(5)	
V [Å^3]	3999(2)	4833(3)
Z	4	4
ρ [g cm^{-3}]	1.535	1.461
μ [cm^{-1}]	0.923	0.774
Crystal size [mm]	0.18 × 0.04 × 0.03	0.20 × 0.20 × 0.20
F(000)	1872	2184
Index ranges	$-18 \le h \le 18$; $-13 \le k \le 14$; $-25 \le l \le 25$	$-13 \le h \le 13$; $-26 \le k \le 26$; $-37 \le l \le 37$
Scan type	phi and omega	phi
$2\Theta_{max}$ [°]/criterion	25.35/>2σI	30.03/>2σI
Param. refined; data/param.	470; 10	562; 19
Reflections collected	12483	13591
Independent reflections	7319	13591
Reflections used	4986	11109
$wR2$	0.0925	0.1036
$R1$	0.0482	0.0428
Flack parameter		−0.042(18)
Goodness of fit	1.000	1.022
Largest diff. peak / hole [e·Å^{-3}]	1.212(.104) / −1.067(.104)	0.486(0.096) / −0.844(0.096)

Table 7. Crystal data and structural refinement details for **14**, **22**

	14	**22**
Empirical formula	$C_{45}H_{41}ClNP_3PdS_2 \cdot CH_2Cl_2$	$C_{45}H_{40}BrNiP_3S_2 \cdot CH_2Cl_2$
M_r	979.59	961.34
T [K]	150.0(1)	150.0(1)
Crystal system	monoclinic	orthorhombic
Space group	$P2_1/n$	$Pna2_1$
a [Å]	9.507(5)	19.445(5)
b [Å]	19.410(5)	23.835(5)
c [Å]	24.136(5)	9.475(5)
β [°]	90.290(5)	
V [Å^3]	4454(3)	4391(3)
Z	4	4
ρ [g·cm^{-3}]	1.461	1.454
μ [cm^{-1}]	0.832	1.710
Crystal size [mm]	0.20 × 0.20 × 0.20	0.18 × 0.12 × 0.04
F(000)	2000	1968
Index ranges	$-13 \le h \le 13$; $-27 \le k \le 24$; $-33 \le l \le 33$	$-26 \le h \le 26$; $-32 \le k \le 32$; $-12 \le l \le 12$
Scan type	phi	phi and omega scans
$2\Theta_{max}$ [°]/criterion	30.03/>2σI	28.70/>2σI
Param. refined; data/param.	480;18	541;17
Reflections collected	21883	11058
Independent reflections	12955	11058
Reflections used	8989	9596
$wR2$	0.1166	0.0945
$R1$	0.0414	0.0399
Flack parameter		0.511(7)
Goodness of fit	1.008	1.009
Largest diff. peak / hole [e·Å^{-3}]	0.356(0.090) / 0.874(0.090)	0.200(0.037) / 0.192(0.037)

density functional theory (DFT) utilizing Becke's three-parameter hybrid method B3LYP.[49,50] The standard 6-311+G(d,p) basis set was used for all atoms (C, H, P, O, N, and S). Harmonic frequencies were calculated at the same level of theory to characterize the stationary points and to determine the zero-point energies (ZPE). Intrinsic reaction coordinates calculations (IRC) were performed to ensure that the transition states found for the (1,2) hydrogen-shift actually connect the two products. Final energies were optimized, including ZPE energies scaled by the empirical factor of 0.9806. All optimized structures reported here have only positive eigenvalues of the Hessian matrix, i.e. they are minima on the potential energy surface. Optimizations of complexes **III**, **IV**, and **V** were also carried out with the hybrid B3LYP functional. The basis set is identical to that used by Frenking and co-workers in many studies.[51] The basis set, which is known as "Basis set II", incorporates the Hay−Wadt small-core relativistic effective core potential[52] and double-ζ valence basis set (441/2111/31) in conjunction with the all-electron 6-31G(d) basis sets for the main-group elements, H, C, O, P, S, Cl.

Inspection of ligand-to-metal donor−acceptor interactions were performed by charge-decomposition analysis (CDA).[53] In the CDA method the (canonical, natural, or Kohn Sham) molecular orbitals of the complex are expressed in terms of MOs of appropriately chosen fragments. In the cases studied the Kohn−Shan orbitals of the B3LYP/II calculations are formed in the CDA procedure as a linear combination of the MOs of the SPS anionic ligand and those of the remaining cationic fragment $[PdCl]^+$ for complexes **IIIa**, **b**. The same method was used to analyze complexes **IVa**, **b**, and **V**, but the two fragments are the neutral ligand $[RP(CH_2PH_2S)_2]$, and the cationic fragment $[PdCl]^+$. In both cases, the ligands and the metal fragments were computed in the geometry of the complex. The orbital contributions are divided into four parts: (i) the mixing of the occupied MOs of the ligand and the unoccupied MOs of the metal fragment. This value (denoted *d*) represents the donation ligand → [metal fragment]; (ii) the mixing of the unoccupied MOs of the ligand and the occupied MOs of the metal fragment. This value (denoted *b*) accounts for the back donation [metal fragment] → ligand; (iii) the mixing of the occupied MOs of the ligand and the occupied MOs of the metal fragment. This term (denoted *r*), which describes the repulsive polarization ligand ⇄ [metal fragment], is negative because electronic charge is removed from the overlapping area of the occupied orbitals; (iv) the residual term (Δ) which results from the mixing of the unoccupied MOs of the two respective fragments. Usually this term is very close to zero for closed-shell interactions. This value constitutes an important probe to determine whether the bonding studied can be really classified as a donor−acceptor interaction following the Dewar−Chatt−Duncansson model. Important deviations from $\Delta = 0$ imply that the bond studied is more conventionally described as a normal covalent bond between two open shell fragments. A more detailed presentation of the CDA method and the interpretation of the results can be found in the literature.[53] CDA calculations were performed with the program CDA version 2.1.[54] These calculations were also performed with the Gaussian-98 program. The charge distributions in the optimized structures were calculated with the NBO partitioning scheme.[55]

Supporting Information Available: ORTEP drawing of compound **5** and geometrical parameters of theoretical structure of **Ia-Ie**, **TSa-TSd**, **IIa−IIe**, **IIIa**, **IIIb**, **IVa**, **IVb**, and **V**.

Acknowledgments

This work was supported by the CNRS, the Ecole Polytechnique and the DGA. M. D. thanks the DGA for financial support. The authors thank IDRIS (Paris XI Orsay University) for the allowance of computer time.

[1] C. J. Moulton, B. L. Shaw, *J. Chem. Soc., Dalton Trans.* **1976**, 1020−1024.
[2] M. Albrecht, G. Van Koten, *Angew. Chem.* **2001**, *113*, 3866−3878; *Angew. Chem. Int. Ed.* **2001**, *40*, 3750−3781.
[3] J. T. Singleton, *Tetrahedron Lett.* **2003**, *59*, 1837−1857.
[4] M. E. van der Boom, D. Milstein, *Chemical Reviews* **2003**, *103*, 1759−1792.
[5] S. Grundemann, M. Albrecht, J. A. Loch, J. W. Faller, R. H. Crabtree, *Organometallics* **2001**, *20*, 5485−5488.
[6] P. Kapoor, A. Pathak, R. Kapoor, P. Venugopalan, M. Corbella, M. Rodriguez, J. Robles, A. Llobet, *Inorg. Chem.* **2002**, *41*, 6153−6160.
[7] A. S. Ionkin, W. J. Marshall, *Heteroatom Chem.* **2002**, *13*, 662−666.
[8] See for example: J. D. Niemoth-Anderson, K. A. Clark, T. A. George, C. R. Ross, *J. Am. Chem. Soc.* **2000**, *122*, 3977−3978.
[9] M. Tschoerner, G. Trabesinger, A. Albinati, P. S. Pregosin, *Organometallics* **1997**, *16*, 3447−3453.
[10] D. A. Evans, K. R. Campos, J. S. Tedrow, F. E. Michael, M. R. Gagne, *J. Am. Chem. Soc.* **2000**, *122*, 7905−7920.
[11] D. R. Evans, M. Huang, W. M. Seganish, E. W. Chege, Y. F. Lam, J. C. Fettinger, T. L. Williams, *Inorg. Chem.* **2002**, *41*, 2633−2641.
[12] X. Verdaguer, M. A. Pericàs, A. Riera, M. J. Maestro, *Organometallics* **2003**, *22*, 1868−1877.
[13] N. Brugat, A. Polo, A. Alvarez-Larena, J. F. Piniella, J. Real, *Inorg. Chem.* **1999**, *38*, 4829−4837.
[14] K. Ortner, L. Hilditch, Y. F. Zheng, J. R. Dilworth, U. Abram, *Inorg. Chem.* **2000**, *39*, 2801−2806.
[15] D. R. Evans, M. S. Huang, W. M. Seganish, J. C. Fettinger, T. L. Williams, *Organometallics* **2002**, *21*, 893−900.
[16] H. Brunner, H. J. Lautenschlager, W. A. König, R. Krebber, *Chem. Ber.* **1990**, *123*, 847−853.
[17] S. M. Aucott, A. M. Z. Slawin, J. D. Woolins, *Eur. J. Inorg. Chem.* **2002**, 2408−2418.
[18] M. J. Baker, M. F. Giles, A. G. Orpen, M. J. Taylor, R. J. Watt, *J. Chem. Soc., Chem. Commun.* **1995**, 197−198.
[19] L. Gonsalvi, H. Adams, G. J. Sunley, E. Ditzel, A. Haynes, *J. Am. Chem. Soc.* **2002**, *124*, 13597−13612.
[20] K. B. Dillon, F. Mathey, J. F. Nixon, *Phosphorus: The Carbon Copy*, John Wiley & Sons, Chichester, **1998**.
[21] M. Doux, C. Bouet, N. Mézailles, L. Ricard, P. Le Floch, *Organometallics* **2002**, *21*, 2785−2788.
[22] M. Doux, N. Mézailles, M. Melaimi, L. Ricard, P. Le Floch, *Chem. Commun.* **2002**, 1566−1567.
[23] P. Le Floch, in *Phosphorus-Carbon Heterocyclic Chemistry: The Rise of a New Domain* (Ed.: F. Mathey), Pergamon, **2001**, pp. 485−533.
[24] N. Mézailles, P. Le Floch, F. Mathey, in: *Progress in Inorganic Chemistry, Vol. 49* (Ed.: K. D. Karlin), John Wiley & Sons, Inc., **2001**, pp. 455−550.
[25] P. Le Floch, D. Carmichael, F. Mathey, *Organometallics* **1991**, *10*, 2432−2436.
[26] See supplementary material available.
[27] See for example: R. Broussier, E. Bentabet, M. Laly, P. Richard, L. G. Kuz′mina, P. Serp, N. Wheatley, P. Kalck, B. Gautheron, *J. Organomet. Chem.* **2000**, *613*, 77−85.
[28] See for example: T. S. Lobana, R. Verma, A. Singh, M. Shikha, A. Castineiras, *Polyhedron* **2002**, *21*, 205−209.
[29] See for example: K. V. Katti, P. R. Singh, C. L. Barnes, *Inorg. Chem.* **1992**, *31*, 4588−4593.
[30] G. Y. Li, *Angew. Chem.* **2001**, *113*, 1561−1564; *Angew. Chem. Int. Ed.* **2001**, *40*, 1513−1515.
[31] N. K. Gusarova, A. M. Reutskaya, N. I. Ivanova, A. S. Medvedeva, M. M. Demina, P. S. Novopashin, A. V. Afonin, A. I. Albanov, B. A. Trofimov, *J. Organomet. Chem.* **2002**, *659*, 172−175.

[32] G. Y. Li, W. J. Marshall, *Organometallics* **2002**, *21*, 590−591.
[33] K. Dimroth, *Acc. Chem. Res.* **1982**, *15*, 58−64.
[34] G. Märkl, A. Merz, *Tetrahedron Lett.* **1971**, *17*, 1215−1218.
[35] A. J. Ashe III, T. W. Smith, *J. Am. Chem. Soc.* **1976**, *98*, 7861−7862.
[36] A. J. Ashe III, T. W. Smith, *Tetrahedron Lett.* **1977**, *5*, 407−410.
[37] G. Märkl, K.-H. Heier, *Angew. Chem.* **1972**, *84*, 1066−1067; *Angew. Chem. Int. Ed. Engl.* **1972**, *11*, 1016−1017.
[38] Z. X. Wang, P. v. Ragué Schleyer, *Helv. Chim. Acta* **2001**, *84*, 1578−1600.
[39] K. Dimroth, A. Hettche, H. Kanter, W. Städe, *Tetrahedron Lett.* **1972**, *9*, 835−838.
[40] A. Moores, L. Ricard, P. Le Floch, N. Mézailles, *Organometallics* **2003**, *22*, 1960−1966.
[41] R. B. King, in *Organometallic Syntheses Academic, Vol. 1*, New York, **1965**, p. 71.
[42] D. Drew, J. R. Doyle, in: *Inorganic Syntheses, Vol. 28* (Ed.: R. J. Angelici), **1990**, pp. 348−349.
[43] M. F. Rettig, P. M. Maitlis, in: *Inorganic Syntheses, Vol. 28* (Ed.: R. J. Angelici), **1990**, pp. 110−111.
[44] J. X. McDermott, J. F. White, J. F. Whitesides, *J. Am. Chem. Soc.* **1976**, *98*, 6521−6528.
[45] A. Altomare, M. C. Burla, M. Camalli, G. Cascarano, C. Giacovazzo, A. Guagliardi, A. G. G. Moliterni, G. Polidori, R. Spagna, *SIR97, an integrated package of computer programs for the solution and refinement of crystal structures using single crystal data*.
[46] G. M. Sheldrick, *SHELXL-97*, Universität Göttingen, Göttingen, Germany, **1997**.
[47] L. J. Farrugia, *ORTEP-3*, Department of Chemistry, University of Glasgow.
[48] M. J. Frisch, G. W. Trucks, H. B. Schlegel, G. E. Scuseria, M. A. Robb, J. R. Cheeseman, V. G. Zakrzewski, J. J. A. Montgomery, R. E. Stratmann, J. C. Burant, S. Dapprich, J. M. Millam, A. D. Daniels, K. N. Kudin, M. C. Strain, O. Farkas, J. Tomasi, V. Barone, M. Cossi, R. Cammi, B. Mennucci, C. Pomelli, C. Adamo, S. Clifford, J. Ochterski, G. A. Petersson, P. Y. Ayala, Q. Cui, K. Morokuma, D. K. Malick, A. D. Rabuck, K. Raghavachari, J. B. Foresman, J. Cioslowski, J. V. Ortiz, A. G. Baboul, B. B. Stefanov, G. Liu, A. Liashenko, P. Piskorz, I. Komaromi, R. Gomperts, R. L. Martin, D. J. Fox, T. Keith, M. A. Al-Laham, C. Y. Peng, A. Nanayakkara, M. Challacombe, P. M. W. Gill, B. Johnson, W. Chen, M. W. Wong, J. L. Andres, C. Gonzalez, M. Head-Gordon, E. S. Replogle, J. A. Pople, *Gaussian Revision A-11 ed.,* Gaussian, Inc., Pittsburgh PA, **1998**.
[49] J. P. Perdew, *Phys. Rev. B.* **1986**, *33*, 8822−8832.
[50] A. D. Becke, *Phys. Rev. A* **1988**, *38*, 3098−3108.
[51] G. Frenking, N. Fröhlich, *Chem. Rev.* **2000**, *100*, 717 −774.
[52] P. J. Hay, W. R. Wadt, *J. Chem. Phys.* **1995**, *82*, 299−310.
[53] G. Frenking, *J. Phys. Chem.* **1995**, *99*, 9352−9362.
[54] S. Dapprich, G. Frenking, CDA 2.1. The program is available online: ftp://chemie. uni-marburg.de (/pub/cda), Marburg, **1995**.
[55] A. E. Reed, L. A. Curtiss, F. Weinhold, *Chem. Rev.* **1988**, *88*, 899−926.

Received May 21, 2003

